Department of Otorhinolaryngology – Head and Neck Surgery
University of Helsinki and University of Turku
Finland

Auger-emitter radiochemotherapy in squamous cell cancers: *in vitro* and *in vivo* experiments with ^{111}In-BLMC

Hilkka Jääskelä-Saari

Academic dissertation

To be publicly discussed, with the permission of the Medical Faculty of the University of Helsinki, in the small auditorium of the Haartman Institute, Haartmaninkatu 3, Helsinki, on August 28th, 2009, at 12 noon.

Helsinki 2009

Supervised by

Professor Reidar Grénman
Department of Otorhinolaryngology – Head and Neck Surgery
Turku University Hospital and University of Turku, Finland

Docent Kalevi Kairemo
Department of Oncology
Helsinki University Central Hospital, Finland

Docent Hans Ramsay
Department of Otorhinolaryngology – Head and Neck Surgery
Helsinki University Central Hospital, Finland

Reviewed by

Professor Matti Anniko
Department of Otorhinolaryngology – Head and Neck Surgery
University Hospital (Akademiska Sjukhuset)
Uppsala, Sweden

Docent Tapani Lahtinen
Department of Oncology
Kuopio University Hospital, Finland

Opponent

Docent Petri Koivunen
Department of Otorhinolaryngology – Head and Neck Surgery
Oulu University Hospital, Finland

ISBN 978-952-92-5792-8 (paperback)
ISBN 978-952-10-5651-2 (PDF)
http://ethesis.helsinki.fi
Helsinki University Print, Helsinki 2009

To
Samuel, Eljas, Alvar, Esko, and Arto

Contents

Abstract

Head and neck squamous cell cancer (HNSCC) is the sixth most common cancer worldwide. Two-thirds of affected patients present with advanced stage III or IV disease. Despite advances in combined modality therapy, involving surgery, radiotherapy, and chemotherapy, the 5-year survival rate remains at 40%. Concomitant external beam radiation and chemotherapy are more effective than radiotherapy alone.

Nuclear medicine utilizes potential radiolabeled carriers in the diagnostics and therapy of cancer. Short-range Auger-electron emitters, such as ^{111}In and ^{114m}In, tagged with a drug, molecule, peptide, protein, new class of trifunctional somatostatin analog or nanoparticles placed in close proximity to nuclear DNA represent a fascinating alternative for treating cancer. In this thesis, we studied the usefulness of ^{111}In-BLMC in the diagnostics and potential therapy of HNSCC using *in vitro* HNSCC cell lines, *in vivo* nude mice, and *in vivo* HNSCC patients.

In vitro experiments with HNSCC cell lines were performed using the 96-well plate clonogenic assay based on limited dilutions. The sensitivity for external beam radiation, BLM, ^{111}In-BLMC, and $^{111}InCl_3$ was studied using several HNSCC cell lines. The influence of BLM and ^{111}In-BLMC on the cell cycle was investigated by flow cytometry.

In *in vivo* nude mice xenograft studies, the activity ratios of ^{111}In-BLMC were obtained in gamma camera images. Another purpose was to examine the effect of ^{111}In-BLMC in HNSCC xenografts. In *in vivo* patient studies, we determined the tumor uptake of ^{111}In-BLMC by gamma camera and the radioactivity and proliferative activity from tumor samples using ^{111}In-BLMC with specific activity of 75, 175, or 375 MBq/mg BLM. The S values, i.e. absorbed dose in a target organ/region per cumulated activity in a source organ/region, were simulated for ^{111}In and ^{114m}In.

In vitro studies expressed the variation of sensitivity for external beam radiation, BLM, and ^{111}In-BLMC between HNSCC cell lines. IC_{50} values for BLM were 1.6-, 1.8-, and 2.1-fold higher than ^{111}In-BLMC (40 MBq/mg BLM) with three HNSCC cell lines. Specific ^{111}In activity of 40 MBq/mg BLM was more effective in killing cells than specific ^{111}In

activity of 195MBq/mg BLM (p=0.0023). $^{111}InCl_3$ alone had no killing effect. The percentage of cells in the G2/M phase increased after exposure to BLM and especially to ^{111}In-BLMC in the three examined cell lines, indicating a G2/M block. Tumor-seeking behavior was shown in the *in vivo* imaging study of xenografted mice. BLM and ^{111}In-BLMC were more effective than NaCl in reducing xenografted tumor size in HNSCC. The uptake ratios received from gamma images in the *in vivo* patient study varied from 1.2 to 2.8 in malignant tumors. However, the uptake of ^{111}In-BLMC was unaffected by increasing the injected activity. A positive correlation existed between ^{111}In-BLMC uptake, Ki-67/MIB activity, and number of mitoses. Regarding the S values, ^{114m}In delivered a 4-fold absorbed radiation dose into the tumor compared with ^{111}In, and thus, the cytotoxicity of Auger-electron therapy might be more effective with ^{114m}In-BLMC than with ^{111}In-BLMC at the DNA level.

Auger-electron emitters, such as ^{111}In and theoretically ^{114m}In, represent an attractive alternative in the treatment of advanced HNSCC. Further studies are needed to develop a radiopharmaceutical agent with appropriate physical properties of the radionuclide and a suitable carrier to bring it near the targeted tissue.

Keywords: HNSCC; Bleomycin; Auger-emitter radionuclide; ^{111}In-BLMC; Chemoradiotherapy

List of original publications

This thesis is based on the following original publications, which are referred to in the text by Roman numerals I-V:

I Jääskelä-Saari HA, Kairemo KJA, Jekunen AP, Pekkola-Heino K, Kulmala J, Ramsay HA, Grénman R. Cytotoxicity of bleomycin and external radiation in squamous cell cancer cell lines of head and neck. Cancer Detect Prevent 20(4):279-284, 1996.

II Jääskelä-Saari HA, Kairemo KJA, Ramsay HA, Grénman R. Labelling of bleomycin with Auger-emitter increases cytotoxicity in squamous-cell cancer cell lines. Int J Radiat Biol 73(5):565-570, 1998.

III Jääskelä-Saari HA, Kairemo KJA, Ramsay HA, Grénman R. Squamous cell cancer cell lines: sensitivity to bleomycin and suitability for animal xenograft studies. Acta Otolaryngol (Stockh) 529:241-244, 1997.

IV Jääskelä-Saari HA, Grénman R, Ramsay HA, Tarkkanen J, Paavonen T, Kairemo KJA. Indium-111-bleomycin complex in squamous cell cancer xenograft tumors of nude mice. Cancer Biother Radiopharm 20(4):426-435, 2005.

V Kairemo KJA, Ramsay HA, Paavonen TK, Jääskelä-Saari HA, Tagesson M, Ljunggren K, Strand S-E. Biokinetics of indium-111-bleomycin complex in head and neck cancer – implementations for radiochemotherapy. Cancer Detect Prevent 21(1):83-90, 1997.

Abbreviations

AC	adenocarcinoma
AUC	area under the curve
BF	benign fibroma
BLM	bleomycin
CHART	continuous hyperfractionated accelerated radiotherapy
CT	computed tomography
D	mean inactivation dose
DI	DNA index
DMEM	Dulbecco´s modified Eagle medium
DNA	deoxyribonucleic acid
EC	ectron capture
ECT	electro-chemotherapy
EDTA	ethylenediamine-tetra-acetic acid
EP	electric pulse
eV	electron volt
FBS	fetal bovine serum
FDG	fluorodeoxyglucose
G0	resting phase of cell cycle
G1	interphase of cell cycle
G2/M	premitotic and mitotic phase of cell cycle
Gy	gray, unit of absorbed dose
HDR	high dose rate
HNSCC	head and neck squamous cell carcinoma
HPF	high-power field
HPV	human papilloma virus
IC_{20-90}	drug concentration causing 20-90% inhibition of clonogenic survival
IC	internal conversion
ICRP	International Commission on Radiation Protection
ID	injected dose
IMRT	intensity modulated radiation therapy

^{111}In-BLMC	indium-111-bleomycin complex
LDR	low dose rate
LET	linear energy transfer
LQ	linear-quadratic
MBq	megabecquerel
MCD	multichannel detector
MIRD	medical internal radiation dose
MRT	mean residence time
NaCl	sodium chloride
NL	neurilemmoma
PDR	pulsed dose rate
PE	plating efficiency
PET	positron emission tomography
RBE	relative biological effectiveness
ROI	region of interest
RTS	relative tumor size
SCC	squamous cell carcinoma
SCID	severe combined immunodeficiency
SCLC	small cell lung carcinoma
SD	standard deviation
SF	survival fraction
SF_2	survival fraction after a single radiation dose of 2 Gy
SPECT	single photon emission computed tomography
S value	absorbed dose in a target organ/region per cumulated activity in source organ/region
$T_{1/2,biol}$	biological half-life
$T_{1/2,eff}$	effective half-life
$T_{1/2,phys}$	physical half-life
T_D	doubling time
TLC	thin-layer chromatography
TNM	tumor, node, metastasis
T/non-T	tumor fraction divided by non-tumor fraction
UICC	International Union Against Cancer

1. Introduction

Head and neck squamous cell cancer (HNSCC) is the sixth most common cancer in the world (Parkin et al. 2005). The International Agency for Research on Cancer estimates that globally HNSCC accounted for more than 600 000 cases in 2002 (GLOBOCAN 2002, Parkin et al. 2005).

In general, surgery or radiotherapy is the main treatment regimen for stage I and II HNSCCs. Worldwide, approximately two-thirds of HNSCCs are in stage III/IV at presentation. Locally advanced HNSCC patients treated with surgery in combination with radiotherapy are known to be at risk of locoregional recurrence in 30% and distant metastases in up to 25% of cases (Laramore et al. 1992, Spector et al. 2001). The 5-year overall survival rate of stage III and IV disease remains at 40%. The addition of chemotherapy concomitantly to radiotherapy has improved patient outcome. Several meta-analyses have been performed comparing concomitant chemoradiation to radiation alone in treatment of advanced HNSCC (Pignon et al. 2000, Bourhis et al. 2007, Pignon et al. 2007). Two large-scale prospective randomized trials comparing concomitant cisplatin and irradiation versus radiotherapy alone demonstrated significant improvement in outcome of concomitantly treated locally advanced HNSCC patients (Bernier et al. 2004, Cooper et al. 2004).

Despite combined-modality approaches, including surgery, external radiation, and chemotherapy, the risk of failure is high. We need tools to prevent local recurrences and eradicate micrometastases (Colnot et al. 2004). A radionuclide tagged with a drug, molecule, peptide, protein, new class of trifunctional somatostatin analog, or a nanoparticle, offers a potential means for diagnostics and therapy of cancer. After 1971, the official inception of nuclear medicine, this field has evolved rapidly (Graham and Metter 2007).

Radioactive isotopes are called radionuclides. They are unstable atoms that disintegrate randomly with the emission of ionizing radiation (Ahonen et al. 2003). They can be produced in many nuclear reactions, and thus, in industrial nuclear reactors and particle accelerators. In 2005, a total of 125 radionuclides were available in the United States, but 20 of them were being compounded under the state-regulated practice of medicine and pharmacy

(Silberstein 2005). The physical characteristics of a radionuclide, including gamma energy and physical half-life, determine its suitability for imaging. Gamma-rays emitting radionuclides, such as ^{99m}Tc, ^{111}In, ^{153}Sm, ^{123}I, and ^{170} Er, may be imaged with a gamma camera (SPECT), while positron emitters, such as ^{11}C, ^{13}N, and ^{15}O, can be identified by positron emission tomography (PET).

In addition to diagnosis of cancer and assessment of treatment response, radionuclide-based techniques allow one to monitor the biodistribution of release and kinetics. The quantitative nature of the images enables the site of receptors in the brain in Alzheimer´s disease, Tourette´s syndrome, and epilepsy to be recognized (Chappell et al. 1993, De Lanerolle et al. 1997, Mathieu-Kia et al. 2001). Radionuclides have been successfully applied to the assessment of myocardial viability, function of kidneys and lungs, and identification of locations of inflammation, atherosclerosis, and thrombosis (Arrighi and Dilsizian 2006, Jalilian et al. 2006). Scintigraphic studies may even be used to examine gastric emptying or ocular pharmacokinetics (Perkins and Frier 2004). The results of radiotargeted gene therapy have been encouraging in animal xenograft models (Buchsbaum 2004, Buchsbaum et al. 2005).

Radionuclide-based therapy requires appropriate physical properties of the radionuclide, a suitable carrier to bring it near the targeted tissue, high affinity and specificity for tumor cells, and a known of radiation decay on the cell cycle and DNA (Kassis 2005, Kassis and Adelstein 2005). Interesting emissions are composed of energetic α- and β-particles or low-energy particles, such as low-energy Auger-electrons.

Van Dongen et al. demonstrated a total ablation of HNSCC and ovarian cancer xenografts treated with an antibody tagged with ^{186}Re (Gerretsen et al. 1993, Kievit et al. 1997). Radioactive cisplatin (^{191}Pt) reduced the tumor size more than cisplatin alone in nude mice (Areberg et al. 2001).

Several preclinical investigations have been done to produce a potent radiopharmaceutical agent for therapy (Börjesson 2003, Börjesson 2004, Perk et al. 2005). Current radionuclide therapy commonly uses β-emitters tagged to a monoclonal antibody. The US Food and

Drug Administration has approved ^{90}Y-ibritumomab tiuxetan and ^{131}I-tositumomab for the treatment of nonHodgkin´s lymphoma (DeNardo et al. 2006).

Several radionuclides such as indium-111 (^{111}In) emit also low-energy Auger-electrons with a short range, from one nanometer up to ~ 0.5 μm, causing chromosome aberrations inside the cell (Sastry and Rao 1984, Hou et al. 1992). Auger-electrons are atomic orbital electrons emitted as an alternative to x-ray emission after electron capture (EC), and they deposit their energy in the vicinity of the decay site (Sorenson and Phelps 1987, Howell 1992). The estimated absorbed dose rate at the center of a cell released by ^{111}In is 18 times higher when the radioactivity impacts the nucleus rather than the cell membrane (Faraggi et al. 1994).

Bleomycin (BLM) is a mixture of chemotherapeutic glycopeptidic antibiotics produced by a strain of Streptococcus verticillus (Umezava et al. 1966a). It binds to DNA, causing single- and double-strand breaks (Kuo and Haidle 1973, Iqbal et al. 1976, Burger et al. 1981, Cheong and Iliakis 1997). BLM may be used in treatment of locally advanced and metastatic HNSCC, especially in combination with such drugs as cisplatin and 5-fluorouracil.

^{111}In tagged to BLM easily forms ^{111}In-bleomycin complex (^{111}In-BLMC) (Thakur et al. 1973). ^{111}In-BLMC is stable *in vitro* and *in vivo* and is not toxic to bone marrow (Hou et al. 1984b). Hou et al. demonstrated in small cell lung cancer cells by autoradiography that ^{111}In-BLMC is localized 78.3% in the nucleus and nuclear membrane (Hou and Maruyama 1992). The anti-tumor effect of ^{111}In-BLMC has been expressed in human small cell lung cancer (SCLC) cell lines (Hou et al. 1989a) and in glioma-bearing nude mice (Hou et al. 1985). ^{111}In-BLMC has a tumor-seeking behavior expressed in patients with HNSCC (Kairemo et al. 1996a) and gliomas (Korppi-Tommola et al. 1999).

This thesis examines *in vitro* and *in vivo* with xenografted mice the antitumor effect of ^{111}In-BLMC in HNSCC. Cellular sensitivity to BLM and external beam radiation was compared to observe possible co-sensitivity and cross-resistance patterns in HNSCC cell lines. In the patient study, mitoses, proliferation, and tumor targeting with ^{111}In-BLMC of three different ^{111}In activities were investigated in HNSCC tissue. Finally, based on human imaging study, a phantom model derived from CT images was built to examine the actual

absorbed radiation doses of ^{111}In-BLMC and ^{114m}In-BLMC, aiming to find a proper radionuclide for radiochemotherapy (Table 1).

Table 1. Summary of study design.

***In vitro* cell models**	***In vivo* models**	***In silico* models**
Generation of radiosensitive cell lines	Generation of radio- and chemosensitive animal tumor model for HNSCC	Building a human phantom with a HNSCC tumor and metastasis model
Generation of chemosensitive cell lines	Growth characteristics	Generation of geometric factors for HNSCC primary and metastasic tumor dosimetry for two radioisotopes

2. Review of the literature

2.1. Epidemiology of head and neck squamous cell cancer (HNSCC)

The majority of HNSCCs (~90%) originate from squamous cell mucosa ranging from poorly differentiated to well-differentiated tumors (Zarbo and Crissman 1988). Keratin or "keratin pearls" in the depths of the epithelium on histological samples are characteristic of SCC (Zarbo and Crissman 1988). Premalignant lesions of HNSCC are erythroplakia (Guggenheimer et al. 1989) and leukoplakia (Walkdron and Shafer 1975). HNSCCs include squamous epithelial malignant tumors arising from the mucosa of the oral cavity, pharynx, larynx, nasal cavity, paranasal sinuses, and salivary glands, and from the skin of the face. HNSCCs are classified according to the TNM (tumor, node, metastasis) staging system established by the International Union Against Cancer (UICC) (Sobin and Wittekind 2002). The status of the lymph nodes of the neck has been shown to be the most important prognostic factor for HNSCC (Leemans et al. 1993, Léon 2000, Spector et al. 2001).

Tobacco smoking is regarded as a significant risk factor for carcinogenesis, especially in oral and pharyngeal cancers (Forastiere and Kock 2001, Warnakulasuriya et al. 2005). High alcohol consumption is another important risk factor for the development of HNSCC (Blot 1992, Licitra et al. 2002, Walker et al. 2003). There is mounting evidence that epigenetic alterations of some genes may be related to the carcinogenetic effect of tobacco and such alcohol metabolites as acetaldehydes (Peters et al. 2005, Kraunz et al. 2006b, Marsit et al. 2006). A hereditary family history of cancer may play a role in the development of HNSCC (Copper et al. 1995, Foulkes et al. 1995). A diet containing low amounts of fresh fruits and vegetables is associated with an increased risk of HNSCC (De Stefani et al. 1999). Low dietary intake of folate is a well-known risk factor for HNSCC (Kraunz et al. 2006a). Human papilloma viruses (HPVs) have been shown to be involved in the carcinogenesis of HNSCC, especially in the oropharynx (Chen et al. 2005, Syrjänen 2005, Fakhry and Gillison 2006).

Worldwide incidence rates of HNSCC vary highly. The age-standardized incidence of laryngeal cancer in northern Europe was 4.3 per 100 000 in men and 0.7 per 100 000 in women in 2002, whereas in southern Europe the corresponding rates were 10.9 and 0.7 per

100 000. The highest incidence of oral cancer, 31.5 per 100 000 men, is found in Melanesia compared with 9.2 per 100 000 men in southern Europe and to 5.3 per 100 000 men in northern countries (GLOBOCAN 2002, Parkin et al. 2005).

According to the Finnish Cancer Registry in 2006, the age-adjusted incidence of HNSCC in men was 10.7 per 100 000. In women, the corresponding figure was lower, 4.4 per 100 000 (Finnish Cancer Registry 2006). The age-adjusted mortality rate of HNSCC per 100 000 in 2006 was 3.1 in men and 1.1 in women.

2.2. Treatment of HNSCC

2.2.1. Surgery

Surgery and radiotherapy are the cornerstones of treatment of early-stage HNSCC (Stage I or II), with locoregional control rates of 70-80%. Advanced stage disease (Stage III or IV) in turn is treated with a combination of surgery and radiation or chemoradiation. Since 1960, the development of reconstructive surgery and particularly during the 1970s the development of pedicle and free flaps were huge leaps forward in the functional outcome of patients. The pectoralis major myocutaneous flap described by Aryian in 1979 is still in use. Progress of surgical techniques, including microsurgery, has rendered it possible to reconstruct large defects in the HNSCC region and get a better functional result.

The presence of a single lymph node on either ipsilateral or the contralateral side of the neck reduces the 5-year survival rate to only half of that for N_0 patients. Modified, selective, or radical neck dissection should be carried out if metastatic lymph nodes are present or if there is more than a 15-20% risk of occult disease (Chin et al. 2006).

Unfortunately, the overall survival for advanced-stage cases at 5 years is still only 30-50% (Chin et al. 2006). More complex management strategies have been developed to improve disease control and survival (St John et al. 2006). However, normal tissue morbidity is an important factor in treatment optimization (Trotti 2000, Bentzen and Dische 2001).

2.2.2. External beam radiotherapy

Radiotherapy as a single modality treatment is a primary treatment form in some early-stage HNSCCs. In addition, an advantage of combined surgery and radiation has been demonstrated, among others, by Fletcher and Evers already in 1970. Radiation therapy is often used after surgery as a curative adjuvant treatment. Developments in radiotherapy delivery have improved the prognosis of HNSCC. However, many patients are still diagnosed when disease has advanced locally or regionally to such an extent that operative treatment is no longer sufficient or feasible. Radiation and medical oncology may still help these patients as a palliative treatment modality.

In conventional fractionated radiotherapy, 1.8-2.0 Gy is given as a single dose 5 days a week to a total dose of 60-70 Gy. Hyperfractionation and accelerated fractionation have been explored as promising types of altered fractionation (Horiot et al. 1992, Horiot et al. 1997, Ang 1998, Bourhis et al. 2004). The concept of hyperfractionation is based on an increased dose-fractionation schedule, keeping the overall treatment time unchanged (Bernier and Bentzen 2003). Smaller fraction doses (< 1.2 Gy) two or three times a day can protect slowly responding normal tissues, enabling the total dose of radiation to be raised by 10-15% (Ang 1998). An increased schedule and a rate of dose-accumulation exceeding 10 Gy a week is classified as accelerated (Bernier and Bentzen 2003). The intention is to compensate with an altered radiation schedule the accelerated repopulation of the surviving clonogenic cells during fractionated radiotherapy (Gibson and Forastiere 2004). With this method, the overall time of radiation therapy is reduced. In continuous hyperfractionated accelerated radiotherapy (CHART), the total dose was reduced to 54 Gy by giving 1.5 Gy/fraction three times a day (4-hour intervals) over 12 days.

The development of computed tomography (CT)-guided three-dimensional conformal radiotherapy planning has created a novel form of therapy, the intensity-modulated radiation therapy (IMRT), which enables more conformal dose distributions. The optimal dose distribution in the target volume allows sparing of normal tissues, decreasing sequelae (Verhey 2002). IMRT schedules have achieved successful results in the treatment of many types of HNSCCs (Chao et al. 2001, Xia et al. 2004, Saarilahti et al. 2005, Tenhunen et al.

2008). Saarilahti et al. (2005) demonstrated how IMRT effectively reduced the absorbed dose to the salivary glands without markedly compromising the received target dose.

2.2.3. Chemotherapy

Since 1970, when the first promising HNSCC patient studies with cytotoxic drugs were performed, chemotherapy has belonged to the treatment regimen of advanced HNSCC (Bernier and Cooper 2005).

Chemotherapy can be given as a single treatment and is then usually used for palliation in HNSCC. In treatment with a curative intent, chemotherapy has been used concomitantly with radiation or as an adjuvant or neoadjuvant therapy.

2.2.4. Concomitant chemoradiotherapy

For improving patient outcome, concurrent chemoradiotherapy has been more effective than neoadjuvant and adjuvant schedules (Eisenberger and Jacobs 1992, Aisner et al. 1994, Bourhis and Eschwege 1996, Pignon et al. 2000, Bernier and Bentzen 2003, Bourhis et al. 2007, Pignon et al. 2007). Chemotherapeutic agents are thought to inhibit the repair of lethal and sublethal damage caused by radiation. They probably also radiosensitize hypoxic cells and synchronize tumor cells into the G2/M, which is the most radiosensitive phase of the cell cycle (Bernier and Cooper 2005).

Pignon et al. (2000) showed in the meta-analyses an 8% survival benefit with concomitant chemoradiotherapy at 2 and 5 years. The benefit of adjuvant or neoadjuvant chemotherapy was modest. Munro (1995) reported in a meta-analysis of 54 randomized controlled trials that single-agent chemotherapy with concomitant radiotherapy increased survival by 12.1% in HNSCC patients.

Adelstein et al. (2000) reported a prospective randomized trial where 100 patients with stage III/IV HNSCC were randomized to receive 1.8-2 Gy radiation per day either without (Arm A) or with (Arm B) concurrent 5-fluorouracil and cisplatin. The 5-year Kaplan-Meier estimates for overall survival for Arms A and B were 48% and 50%, respectively,

but a significant benefit of 11% in 5-year recurrence-free interval and 9% in distant metastasis-free interval was observed.

In a study by Forastiere et al. (2003), 547 stage III/IV HNSCC patients were randomized to three arms: induction cisplatin and 5-fluorouracil followed by radiation 2 Gy/day (Arm A), concurrent cisplatin and radiotherapy (Arm B), or radiotherapy alone (Arm C). Total laryngectomy was used as an indication of failure of organ-sparing treatment. At 2 years, locoregional control for Arms A, B, and C was 61%, 78%, and 56%, respectively. Chemotherapy reduced the development of distant metastasis by 8-9% compared with radiotherapy alone. However, no benefit in overall survival was demonstrated.

Two independent, large-scale, prospective randomized trials were published in 2004. In the study by Cooper et al. (2004) after resection of macroscopic HNSCC, 459 patients were randomized to receive either radiotherapy (Arm A) or radiotherapy plus concurrent cisplatin (Arm B). The locoregional control at 2 years was 72% in Arm A versus 82% in Arm B. Disease-free survival was longer in Arm B than in Arm A, but overall survival did not differ significantly. The acute adverse effects of grade 3 or greater, e.g. hematologic complications, vomiting and upper gastrointestinal tract problems, were observed in 34% of patients in Arm A and in 77% of patients in Arm B. In the study by Bernier et al. (2004), after curative surgery, 167 HNSCC patients were treated with either radiotherapy (Arm A) or radiotherapy with simultaneous cisplatin (Arm B). The Kaplan-Meier estimates for 5-year progression-free survival in Arms A and B were 36% and 47%, and for overall survival 40% and 53%, respectively. Grade 3 or greater acute adverse effects were registered in 21% of patients in Arm A and in 41% of patients in Arm B.

2.2.5. Brachytherapy

Before the widespread use of megavoltage external beam radiotherapy for HNSCC in the 1960s, brachytherapy (BT) with radioactive isotopes together with surgery and orthovoltage x-rays were used for the treatment of head and neck cancers. BT was used as a primary treatment, but also for the management of previously irradiated recurrent or new primary tumors or neck metastases (Pernod et al. 1996, Nutting et al. 2006). After the 1960s, the most applied radioisotope has been ^{192}Ir due to its mean gamma energy of 360 keV, half-

life of 74 days, and low cost. One of the most popular implantation techniques was the so-called plastic tube technique, where the thin, coiled platinium-coated ^{192}Ir-wire was cut into suitable lengths and implanted inside the plastic tubes inserted into the tumor under local or general anesthesia. The technique was called manual afterloading. Since a typical dose rate in tumors was 10 Gy/day, 6 days were required to reach the curative dose of 60 Gy in SCC. These techniques necessitated well-trained personnel, and the biggest disadvantage was radiation exposure of personnel to the handled radioisotopes.

In 1970-1990, a device-based afterloading was developed and HNSCC tumors could be treated also with low dose rate (LDR), high dose rate (HDR), and pulsed dose rate (PDR) BT (Nath 1993, Puthawala et al. 2001, Ding et al. 2005, Grimard et al. 2006). Plastic tubes were inserted into tumors as in manual afterloading, but now the automated electronic devices, called afterloaders, were attached to these tubes. Based on the treatment planning and prescribed dose, the afterloaders were programmed to send a single very high-activity source, typically ^{137}Cs, ^{60}Co, or ^{192}Ir, to these tubes. The source moved step-wise inside the tube, irradiating the tumor. The treatment times were minutes to hours, as compared with days with manually afterloaded ^{192}Ir LDR BT. Due to limited tolerance of nearby healthy tissues, the dose needed to destroy the tumor could be not delivered in a single treatment. Therefore, the treatment was fractionated, i.e. given in several smaller fractions. Recently, implants containing radionuclides with different half-lives instead of a single source have been suggested for further improvement of therapeutic effect (Chen and Nath 2003). The long-term results of HDR BT have been similar to those of manually afterloaded LDR BT (Nose et al. 2004). Within the last 20 years, PDR BT has partly replaced the manually afterloaded ^{192}Ir-wire and plastic tube technique since radiation exposure of personnel can be completely avoided.

2.3. Bleomycin

Bleomycin (BLM) is a mixture of structurally related glycopeptide antibiotics, originally isolated from a strain of Streptomyces verticillus (Umezawa et al. 1966a, Umezawa et al. 1966b). BLM is a polypeptide that has three different functional parts: 1) galactos or mannos derivatives, which are thought to detect tumor cells, 2) a metal-chelating part, which

activates the metal bound to the molecule to destroy or damage the tumor, 3) a terminal part, which has variable terminal amino acids causing splitting of tumor DNA.

The BLM-iron complex produces oxygen radicals that bind to nuclear DNA, causing single- and double-strand breaks (Kuo and Haidle 1973, Fujimoto 1974, Lown and Sim 1977, Povirk et al. 1989, Cheong and Iliakis 1997), and kills dividing cells mainly in the G_2 and M phase (Barranco et al. 1973a, Barlogie et al. 1976). In a phase-specific schedule by Barranco et al. (1971) radiomimetic BLM acted as a cell-synchronizing agent and blocked reversibly the cells in G_2 phase in Chinese hamster ovary cells *in vitro*. Despite cell-cycle phase specificity, BLM is not less active in plateau phase than in logarithmic growing cells (Barranco et al. 1973b). However, cell-synchronizing G_2 phase block findings of BLM have generally not been confirmed (Wenneberg 1984, Wahlberg 1987). The plasma half-life of BLM is 2-4 hours, and it is eliminated mainly by urinary excretion (Alberts et al. 1978). About 50% of the drug is excreted intact in the urine and the remainder undergoes metabolism (Dorr 1992). BLM does not accumulate in the liver, spleen, intestine, or bone marrow, all of which have high intrinsic hydrolase activities (Ohnuma et al. 1974, Kramer et al. 1978). BLM hydrolase, which hydrolyzes the terminal carboxamide group of the beta-aminoalanine moiety of the BLM molecule, converts BLM into an inactive desamino form, probably explaining the primary mechanism of BLM resistance (Lazo et al. 1982, Septi et al. 1991). Another potential mechanism may be elevated DNA repair activity (Iqbal et al. 1976, Dar and Jorgensen 1995, Sasiadek et al. 2002).

In vitro BLM has cytotoxicity against several cancer cell types, including squamous cell carcinoma (SCC). Considerable, even ten-fold (Urade et al. 1992) differences in sensitivity for BLM have been demonstrated between SCC cell lines, whereas differences in radiosensitivity for external radiation are not as large (Grénman et al. 1988b, Grénman et al. 1991).

BLM is not detrimental to bone marrow function and causes little nausea and vomiting. More than half of patients experience fever and about half of patients suffer some mucocutaneous toxicity effects. Less frequently, BLM causes pneumonitis and lung fibrosis, which can be fatal in 1-2% of cases.

Clinically, BLM has been administered in combination therapies to patients with testicular cancer, some nonHodgkin´s lymphomas, Kaposi´s sarcoma, head and neck cancer, and cervical cancer.

Shanta and Krishnamurthi (1980) demonstrated a 65.5% five-year survival rate for treatment of oral cancer with BLM combined with radiation compared with 23.5% for radiation alone. In a randomized trial of 104 stage III or IV HNSCC by Fu et al. (1987), patients received either radiotherapy alone (Arm A) or radiotherapy with BLM and methotrexate (Arm B). The 2-year locoregional control rate and the proportion of distant metastases were 26% and 24% in Arm A vs. 64% and 38% in Arm B. However, no significant differences were present in overall survival curves. In a trial by Smid et al. (2003), 114 HNSCC stage III or IV patients were randomized to receive either postoperative radiotherapy (Arm A) or radiotherapy combined simultaneously with mitomycin C and BLM (Arm B). The locoregional control at 2 years was 69% in Arm A and 86% in Arm B. The disease-free survival was 16% higher and the overall survival 10% higher in the chemoradiotherapy group than in the radiotherapy group.

2.4. Radionuclides

Becquerel discovered radioactivity as early as 1896. Since 1971, nuclear medicine has evolved dynamically (Graham and Metter 2007, Murdoch and Sager 2008). Many clinically used radionuclides have fallen out of favor, e.g. ^{81m}Kr for ventilation imaging and ^{99m}Tc-albumin microspheres for lung perfusion, while other agents, e.g. ^{18}F combined with FDG, appear promising (Graham and Metter 2007).

Radionuclides emit gamma-rays, characteristic x-rays, and charged particles. Gamma-rays have no mass or electrical charge, and they travel at the velocity of light. In interactions between high-energy gamma-rays and matter, only a fraction of the energy of gamma-rays will be absorbed. The interactions create electrons, which in turn cause ionization effects (Johns and Cunningham 1983, Sorenson and Phelps 1987). As a consequence of these interactions, high-energy photons are detected, and they result in radiobiological effects. Generally, radionuclides at a high specific activity are needed for therapeutic purposes.

Gamma-ray emitters, such as ^{99m}Tc, ^{111}In, and ^{123}I, may be imaged with a single-photon emission computed tomography (SPECT), and positron-emitters, such as ^{18}F and ^{11}C, are imaged with positron emission tomography (PET) (Ahonen et al. 2003, Perkins and Frier 2004).

In radionuclide therapy, interesting radiations are particulate, e.g. α-, β-, or low-energy particles, such as Auger-electrons, while in external beam radiotherapy high-energy photons or electrons are used (Kassis and Adelstein 2005). Alpha-emitters with their high linear energy transfer (LET) and short path length are suitable for targeting hematopoietic cells, whereas beta-emitters, such as ^{186}Re, ^{67}Cu, ^{131}I, and ^{90}Y, are more suited to solid tumors because of their lower energy and longer path length (Bethge and Sandmaier 2005). In certain medullary thyroid carcinomas, high activities (7.4-11.1 GBq) of ^{131}I have been proposed again as an adjuvant therapy to total thyreoidectomy (Erdogan et al. 2006, Rufini et al. 2008). β-particles destroy cells within a radius of 12 mm. The US Food and Drug Administration has approved ^{90}Y-ibritumomab tiuxetan and ^{131}I-tositumomab for the treatment of nonHodgkin´s lymphoma (DeNardo et al. 2006).

Auger-electron emitters, such as ^{123}I, ^{125}I, and ^{111}In, emit low-energy Auger-electrons which extend from one nanometer to ~ 0.5 μm and are locally absorbed. A few Auger-emitters are presented in Table 2 (ICRP 1983, Howell 1992, Kassis and Adelstein 2005). The linear energy transfer (LET) of the Auger-electrons is more than 20-fold higher than the LET observed with energetic β-particles. The electrons of beta decay can extend to ~ 12 mm and are also locally absorbed (Kassis and Adelstein 2005). The use of therapeutic β-particles requires the presence of very high radionuclide concentrations within the targeted tissue. Auger-electron emitters represent an attractive alternative to beta-emitters for cancer therapy if they can be located with a proper tracer close to the nuclear DNA (Bodei et al. 2003).

Table 2. Auger-electron emitters.

Radionuclides	Half-life	β-particles *	Auger-electrons
^{77}Br	57 h	7	7
^{123}I	13.3 h	11	8
^{125}I	59.4 days	20	8
^{111}In	2.8 days	15	8
^{114m}In	49.5 days	0	5
^{195m}Pt	4 days	36	8

* Average number of β-particles per decay

2.5. The Auger process

When an electron from the inner shell of certain radioactive atom is removed as a consequence of internal conversion (IC) and/or electron capture (EC), an electron from an outer shell immediately fills an inner shell vacancy. The released energy is emitted as characteristic x-rays or another outer shell orbital electron takes the energy. In this latter Auger process, the electron called an Auger-electron is then emitted from the atom instead of characteristic x-rays (Sorenson and Phelps 1987). ^{111}In emits on average 15 β-particles and 8 very short-range Auger-electrons (Howell 1992). Each inner shell electron removal leads to characteristic x-rays or Auger-electrons. Generally, an atom emits 5-30 Auger-electrons with energies from a few eV to 1 keV (Kassis 2005). When the Auger-electrons deliver their energy, the absorbed dose in the decay site within a radius of a few nanometers is of the order of $10^4 – 10^7$ Gy (Kassis and Adelstein 2005).

2.6. Relative biological effectiveness

The International Commission on Radiation Protection (ICRP) formulated the definition: "The Relative Biological Effectiveness (RBE) of radiation A with respect to reference radiation R is defined as the ratio of absorbed dose D_R in a tissue to the dose D_A that causes a quantitatively and qualitatively equal effect. Each RBE value derived from a set of observations for tissue cultures of responses of tissues, in animals or in man, refers to a defined end-point, produced under a specified set of exposure conditions" (ICRP 1979). RBE val-

ues are dependent strongly on the end-point and reference radiation. Earlier, the reference radiation was usually 250-keV x-rays. Nowadays, an equivalent dose of ^{60}Co gamma-rays or radiation produced in the linear accelerators is easily available. The effectiveness of producing biological damage by incorporated radionuclides depends on the nature and energy of the radiations as well as on the biokinetics and the subcellular distribution of the radionuclides (Howell et al. 1993). Faraggi et al. (1994) demonstrated that the absorbed dose rate at the center of the cell is 18 times higher if radioactivity of ^{111}In is localized within the cell nucleus than if it is situated on the cell membrane. When Auger-emitters are situated outside or in the cytoplasm of the cell, low-LET radiation effects are shown, RBE being about one (Rao et al. 1990, Rao et al. 1991). Auger-electron-emitting radionuclides corporated into DNA in the cell nucleus produce high-LET-type effects, with an RBE value of ~ 7-9. *In vitro* and *in vivo* experiments with Auger-emitter ^{111}In, which was localized in the cell nucleus via the radiochemical ^{111}In-oxine, but did not bind to DNA, produced an RBE value of ~ 4 (Rao et al. 1988, McLean et al. 1989). RBE has been reported to be 7.3 with DNA-incorporated ^{125}I compared with the corresponding value from 250 keV x-rays for the same cell line (Kassis et al. 1987a). When the decay of ^{125}I is localized in the cytoplasm, RBE is ~ 1.3, as in the case of equivalent amounts of beta or gamma emission. The DNA-binding ^{125}IdU is about 1.6 times more cytotoxic to V79 cells than 5.3 MeV α-particles from intracellular ^{210}Po-citrate (Howell et al. 1991).

2.7. ^{111}In-BLMC

^{111}Indium is an Auger-emitter with a half-life of 2.8 days. ^{111}In emits gamma-rays, characteristic x-rays, β-particles, and Auger-electrons. ^{111}In easily forms a complex with BLM (Thakur et al. 1973). ^{111}In-BLMC is stable *in vitro* and *in vivo* and because it does not bind to transferrin it does not cause toxicity to bone marrow (Hou et al. 1984a, Hou et al. 1984b). Up to 95% of ^{111}In complex activity is excreted via urine within 22 h (Hiltunen et al. 1990). ^{111}In-BLMC has been observed to be a tumor-targeting agent in HNSCC, thus being a useful tracer (Kairemo et al. 1994, Kairemo et al. 1996a, Kairemo et al. 1996b). Tumor-seeking behavior has also been expressed in gliomas (Korppi-Tommola et al. 1999).

In an autoradiography study by Hou and Maruyama (1992), 78.3% of ^{111}In-BLMC was localized in the nucleus and nuclear membrane of human small cell lung cancer (SCLC)

cells. ^{111}In-BLMC induced more chromosome aberration than BLM (Hou et al. 1992). The cytotoxicity of ^{111}In-BLMC has been demonstrated in human small SCLC cell lines (Hou et al. 1989a, Hou et al. 1989b). Moreover, in glioma-bearing nude mice, ^{111}In-BLMC diminished tumor size better than BLM (Hou et al. 1985).

2.8. Positron emission tomography (PET)

PET is a quantitative imaging modality, that allows observation of metabolic tissue activity, proliferation, and blood flow (Chin et al. 2006). Glucose metabolism is increased in malignant tumors. For example, the uptake of fluorodeoxyglucose (FDG) labeled with a positron-emitting 18-fluorine isotope (^{18}F) can be detected by PET (Schmid et al. 2003). At present, ^{18}F-FDG-PET is used to detect primary or unsuspected metastatic tumors in clinical practice (Goerres et al. 2004).

3. Aims of the study

The purpose of this study was to investigate the suitability of Auger-emitter ^{111}In-labeled BLM for diagnosis and potential therapy of HNSCC using *in vitro* HNSCC cell lines and *in vivo* nude mice and human HNSCC patients.
Specific aims were as follows:

1. To study the response of HNSCC cells to BLM and external beam radiation.

2. To compare the toxicity of Auger-emitter ^{111}In-BLMC with BLM and $^{111}InCl_3$ in HNSCC cell lines.

3. To investigate wheather the increase of ^{111}In activity in ^{111}In-BLMC enhances the cytotoxic effect by comparing two specific activities of ^{111}In-BLMC [40 MBq/mgBLM (low) and 195 MBq/mgBLM (high)].

4. To examine the influence of BLM and ^{111}In-BLMC on the cell cycle of HNSCCs.

5. To study the xenografted tumor uptakes of ^{111}In-BLMC.

6. To evaluate whether BLM, especially ^{111}In-BLMC, is toxic and effective *in vivo* in SCC xenografted mice.

7. To determine tumor uptakes of ^{111}In-BLMC and proliferative activities in patient data.

8. To compare geometric factors of radionuclide dose distribution (S values, the absorbed dose in a target organ/region per cumulated activity in a source organ/region) for both ^{111}In and $^{114\,m}$In using the Monte Carlo method.

4. Materials and methods

4.1. Cell lines (I-IV)

The squamous carcinoma cell lines used were obtained from HNSCC patients treated at the Department of Otorhinolaryngology – Head and Neck Surgery, Turku University. The technique has been described in detail elsewhere (Pekkola-Heino et al. 1991, Pekkola-Heino et al. 1992a, Lansford et al. 1999). Tumor site, TNM classification, specimen site, type of lesion, and earlier therapy are presented in Table 3.

The SCC cells were maintained in Dulbecco´s modified Eagle medium (DMEM) containing 2 mM L-glutamine, 1% nonessential amino acids, 100 U/ml penicillin, 100 μg/ml streptomycin, and 10% fetal bovine serum (FBS). The cells were cultured at 37°C in 5% CO_2 in a water vapor-saturated atmosphere. The exponential growth of the cells was ensured by passing the cells at least weekly.

Table 3. Tumor site, TNM classification (UICC), specimen site, type of lesion, and previous therapy of HNSCC patients.

Cell line	Tumor site	TNM	Specimen site (type)	Previous therapy
UT-SCC-2	Floor of mouth	$T_4N_1M_0$	Oral mucosa (P)	None
UT-SCC-8	Supraglottic larynx	$T_2N_0M_0$	Larynx (P)	Radiation
UT-SCC-9	Glottic larynx	$T_2N_0M_0$	Neck (M)	Radiation
UT-SCC-12A	Skin of nose	$T_2N_0M_0$	Skin (P)	None
UT-SCC-12B	Skin of nose	$RT_0N_1M_0$	Neck (M)	
UT-SCC-19A	Glottic larynx	$T_4N_0M_0$	Larynx (P)	None

P = primary tumor, M = metastasis

4.2. Bleomycin (BLM) (I-IV)

BLM was purchased from Lundbeck Co. (Copenhagen, Denmark) containing 68% fraction A2, 30% fraction B2, and 2% other subunits. The stock solution (1 mg/ml) of BLM was prepared in calcium- and magnesium-free balanced salt solution and and stored at -20°C.

4.3. ^{111}In-BLMC (II,IV,V)

Radionuclide ^{111}In was chosen for the studies because one of the coauthors (Kalevi Kairemo) had performed biodistribution experiments with ^{111}In-BLMC. ^{111}In-BLMC with specific activity of 40, 46, 100, or 195 MBq/mg BLM was purchased from MAP Medical Technologies Ltd. (Tikkakoski, Finland). At least 98% of ^{111}In activity was bound to BLM.

Preparation of ^{111}In-BLMC is reported elsewhere in detail (Hiltunen et al. 1990, Kairemo et al. 1996a). Briefly, the complex was prepared by incubating BLM sulfate dissolved in water (2 mg/ml) with $^{111}InCl_3$ at pH 2-2.5 for at least 30 min. The pH was adjusted with an acetate buffer to 6.0.

^{111}In-BLMC was controlled by using thin-layer chromatography (TLC). The composition of radiolabeled BLM was studied in detail by separating different BLM fractions first by TLC and then by gel chromatography.

4.4. $^{111}InCl_3$ (II)

$^{111}InCl_3$ was purchased from Amersham International plc (Little Chalfont, England). The ^{111}In activity was 370 MBq/ml.

4.5. Clonogenic assay (I-III)

The experiments with HNSCC cells were performed using the 96-well plate clonogenic assay. This technique based on limiting dilutions has earlier been described in detail (Grénman et al. 1988a, Grénman et al. 1989). Twenty-four hours before plating, the cells were fed with fresh medium. The cells in mid-logarithmic growth (40-60% confluence)

were harvested with trypsin-EDTA (315 U/ml trypsin and 0.2 M EDTA) and counted with a Bürger chamber after passage through a 25-gauge needle. The cells in Ham´s F-12 medium with 15% FBS were plated immediately onto 96-well plates and moved to a water incubator (37°C, 5% CO_2) for a day, as described earlier (Grénman et al. 1988a, Grénman et al. 1989). Two to three independent experiments were performed with duplicate plates from each cell line for each data point.

In Study I, the cells were irradiated or exposed to given concentrations of BLM. The plates were irradiated with four MeV photon irradiation at a dose rate of 2.00 Gy/min using total doses of 0.75, 1.25, 2.50, and 5.00 Gy in all cell lines and additionally 7.50 Gy in four of the cell lines. The dilutions (1.5-100 nM) of BLM were prepared in the growth medium before use.

In Study II, chosen concentrations of BLM (1.5-100 nM) and ^{111}In-BLMC (40 or 195 MBq/mgBLM), at concentrations corresponding to the BLM concentrations, and $^{111}InCl_3$, were added to the 96-well plates. The ^{111}In activity in $^{111}InCl_3$ corresponded to the ^{111}In activity of ^{111}In-BLMC (40 MBq/mgBLM).

In Study III, various concentrations of BLM (1.5n-100nM) were added to the 96-well plates.

In all experiments, the plates were incubated for four weeks, and living colonies containing at least 32 cells were counted using an inverted phase-contrast microscope.

4.6. Xenograft tumors (III,IV)

UT-SCC-12A and UT-SCC-19A cell lines were injected using 10^7 cells per site subcutaneously into the flank of 6- to 8-week-old balb/c male nude mice (Harlan Laboratories, Great Britain). Nude mice were weighed and settled down in micro-isolators with water and food.

4.7. *In vivo* imaging using a gamma camera (IV,V)

Animals

Tumors of cell line UT-SCC-12A or UT-SCC-19A were grown in the flank of two 6- to 8-week-old balb/c male nude mice for gamma camera imaging.

Two xenografted mice were imaged using a Picker Prism 2000 XP single-photon emission computed tomography (SPECT) gamma camera equipped with a parallel-hole, medium-energy collimator (Picker International, Cleveland, OH, USA). A 256 x 256 x 16 matrix size was used, and gamma energies of ^{111}In 173 keV and 247 keV with 20% windows were recorded.

The UT-SCC-19A xenografted mouse was imaged at 1, 4, 20, 44, and 95 h after an intraperitoneal ^{111}In-BLMC injection (7.77 MBq/mouse). Planar images of the mouse bearing a UT-SCC-12A tumor (904 mm^3) were taken 8, 24, 48, and 100 h after injection of ^{111}In-BLMC. The tumor and the whole body were outlined as regions of interest (ROI), and a nontumor ROI was drawn on the contralateral side of the mouse. Activity ratios, total counts of the tumor divided by total counts of the whole body (T/w-body), and total counts of the tumor in relation to total counts of nontumor regions (T/non-T) were calculated.

Patients

All patients were generally imaged three times, usually at 1, 4, and 20-24 h after injection. A gamma camera (Picker Prism 1500 XP) was used. The matrix size was 128 x 128 x 16, and a medium energy collimator for both energy peaks of ^{111}In (173 keV and 247 keV; 20% windows) was used.

4.8. Experimental therapeutic trial (IV)

The weight of nude mice was 22.7-24.8 g at the beginning of the experiment. Nude mice (n=8) with one xenograft tumor each (14-51 mm^3) were divided into three groups. The tumor volumes in the control group were 14, 16, 23, and 39 mm^3; this group received physiological NaCl intraperitoneally. The tumor volumes were 25 and 39 mm^3 in the BLM group receiving 0.0662 mg BLM/g and 27 and 51 mm^3 in the ^{111}In-BLMC group receiving ^{111}In-BLMC containing 0.0662 mg BLM/g. The treatments were given 6 times over 24 h. The total doses were as follows: 0.0126 mg BLM/g every 4 h, 8 h later 0.0081 mg BLM/g

at 4-h intervals. In the ^{111}In-BLMC group, the administered total activity was 3.063 MBq/g.

The nude mice were weighed and the tumor volumes were measured for 14 days two times a week in three perpendicular diameters and calculated according to the ellipsoid formula ($V=\pi/6*a*b*c$). Tumor volume at the time of measurement in relation to tumor volume at time of injection (relative tumor size, RTS) was calculated for every measurement occasion. The logarithmic values were plotted as a function of time.

After the therapy study, pieces of the tumors were frozen in liquid nitrogen for further flow cytometric analysis and the rest of the tumors were fixed in formalin and embedded in paraffin for histopathologic and proliferative activity studies.

4.9. Histopathology and proliferative activity (IV)

A section of each tumor was stained with hematoxylin and eosin for histopathological diagnosis and the counting of mitoses. The mitoses were scored as follows: (1) if <2/high power field (HPF), (2) if 2-5/HPF, and (3) if >5/HPF.

Staining with rabbit anti-human Ki-67 antigen antibody (dilution 1:150; DAKO, Denmark) was performed according to the avidin-biotin complex method as described elsewhere (Hsu et al. 1981). More than 1000 cells in at least three fields of magnification x400 (HPF) were counted, and positive cells were expressed as a percentage of the total SCC cells. The results were scored on a relative scale from 0 to 3 as follows: (0) if 0%, (1) if <15%, (2) if 15-50%, and (3) if >50%.

4.10. DNA flow cytometry (IV)

This technique has been described in detail in Study IV. Briefly, single-cell suspensions of cell lines UT-SCC-2, UT-SCC-12A, and UT-SCC-19A were plated onto 6-well plates (2 x 10^4 cells/plate). In addition to control medium cultures, measurements of DNA content were performed 24 and 48 h after exposure to BLM (100 nM) and ^{111}In-BLMC (100 nM). Stained nuclei with propidium iodide were analyzed in a FACScan flow cytometer (Becton Dickinson Immunocytometry Systems, Mountain View, CA), with chicken and trout red

blood cells as internal control cells (Alanen et al. 1989). The percentage of phases G0/G1, S, and G2/M of the cell cycle was calculated by MultiCycle software (Phoenix Flow Systems, San Diego, CA, Autofit version 2.50). DNA histograms of at least 14 000 cells were plotted, and a DNA index (DI) was defined to demonstrate DNA ploidy status.

DNA flow cytometry was performed for UT-SCC-12A xenografted tumor samples stored in nitrogen liquid. Generally, at least 8000 cells were measured per histogram. The DI and the total S phase were defined.

4.11. Data analysis (I-IV)

The plating efficiency (PE) was calculated using the formula PE = - ln (number of negative wells/total number of wells)/number of cells plated per well (Thilly et al. 1980).
The survival fraction (SF) was calculated as follows:

$$SF = \frac{\text{(no. of positive wells/no. of plated cells) x no. of plated cells in control}}{\text{no. of positive wells in control}} \quad (1)$$

SFs as a function of BLM concentration or radiation doses were fitted by the linear quadratic equation $F= e^{-(\alpha D+\beta D^2)}$ using a micro-computer program. The area under the survival curve (AUC) value, equivalent to the mean inactivation dose (D), was obtained by numerical integration. Comparison of chemosensitivity was made using 50% values from the dose-response curves (50% inhibition of surviving fraction).

Two to three independent experiments using duplicate plates for each cell line were performed to determine mean and standard deviation (SD) of IC_{20}, IC_{50}, IC_{90}, AUC, and SF_2 values.

In Study II, null and alternative hypotheses were tested using a paired t-test. P-values were certified by Wilcoxon´s signed-rank test. IC_{50} values were calculated from 14 duplicate experiments.

In Study III, the doubling time of the xenograft was determined after fitting an exponential equation $V = k_1 e^{k_2 t.}$ to the dynamic tumor volume data.
The doubling time $T_D = (t_2-t_1)\ \ln 2/(\ln V_2-\ln V_1)$ was calculated from the fitted curve, where V_2 and V_1 are volumes at t_2 and t_1, respectively.

4.12. Patients (V)

Diagnosis and origin of the 10 head and neck tumors used and injected activity of ^{111}In-BLMC are shown in Table 4. Blood and urine samples were collected at regular intervals after injection to estimate clearance of radioactivity.

Table 4. Tumor characteristics in patients.

Patient/Age/Sex	Diagnosis	TNM classification (UICC)	Organ	Tumor size (mm)	Injected activity (MBq)
1. 68/M	SCC	$T_2N_1M_0$	Tonsil (P) Neck (M)	10x10x10 20x15x20	75
2. 68/M	SCC	$T_2N_0M_0$	Larynx, subglottic (P)	10x20x20	175
3. 76/F	SCC	$T_2N_0M_0$	Tongue, base (P)	8x30x15	75
4. 67/M	SCC	$T_0N_3M_0$	Unknown (P) Neck (M)	 60x40x40	75
5. 63/M	SCC	$T_4N_2M_0$	Larynx, transglottic(P) Neck (M)	20x25x15 20x15x15	75
6. 71/F	AC	$T_xN_2M_0$	Eyelid (P)[a] Neck (M)	 23x19x23	175
7. 58/F	BF	-	Maxilla	20x15x15	175
8. 68/M	NL, malignant	$T_2N_0M_0$	Larynx, supraglottic(P)	20x30x30	375
9. 79/F	SCC	$T_2N_1M_0$	Buccal mucosa (P) Neck (M)	48x30x30 18x14x14	375
10. 44/M	SCC	$T_2N_0M_0$	Tongue (P)	16x9x9	375

SCC = Squamous cell carcinoma; AC = Adenocarcinoma; BF = Benign fibroma; NL = Neurilemmoma; P = Primary tumor; M = Metastasis.

[a] Previously removed.

4.13. Surgery and tumor samples (V)

Tumor samples for radioactivity counting were obtained from operations performed approximately 48 h after the intravenous injection of ^{111}In-BLMC. Radical tumor removal was achieved in all cases. These operations included seven radical or modified neck dissections, two hemiglossectomies, three partial or total laryngectomies, and three local tumor excisions.

Samples of tumor and normal tissues obtained at surgery were processed further while fresh. Pieces of the samples were fixed in formalin and embedded into paraffin for histopathological van Gieson and hematoxylin-eosin staining. Fresh tissue samples were weighed and radioactivity was counted using an ^{111}In internal standard (LKB 1282 Compugamma; Wallac, Turku, Finland). Samples for immunohistochemistry were prepared in Histostix and fast-frozen using liquid nitrogen. Thick sections of the samples were stained immediately or stored at -20^0C.

4.14. Proliferative activity (V)

The proliferative activity was determined by counting the number of mitoses and Ki-67–positive cells. For analysis, monoclonal antibody MIB-1 against nuclear antigen Ki-67 was purchased from Immunotech S.A. (Marseilles, France). A 1:50 dilution of MIB-1 antibody was used in an immunoperoxidase technique with avidin-biotin conjugates (Paavonen and Renkonen 1992). The frequencies of mitosis and MIB-1 reactivity were scored on a relative scale from (1) to (3) as follows: for mitosis activity: (1) if <2/high power field (HPF), (2) if 2-5/HPF, and (3) if >5/HPF, for MIB activity: (0) if 0%, (1) if <15%, (2) if 15-50%, and (3) if >50%.

4.15. Monte Carlo simulation and phantom studies (V)

A Monte Carlo program was originally developed as part of a scheme for systemic radiation treatment, based on quantitative SPET (Ljungberg et al. 1994a, Ljundberg et al 1994b, Tagesson et al. 1996). By means of anatomical and isotope images, the program simulates photons by following each photon from the decay of the radionuclide until the photon either undergoes photoelectric absorption or escapes the phantom/patient, or the photon en-

ergy drops under a certain cut-off point. In Study V, all regions of interest were larger than the electron range, and the electrons were considered locally absorbed. S values for arbitrary geometries and all radionuclides may be calculated according to this Monte Carlo program.

Kairemo et al. (1996b) earlier calculated S values of different isotopes of indium (^{111}In, ^{111m}In, ^{113m}In, ^{114}In, ^{114m}In, and ^{115m}In) for spherical tumors from the tabulated data in MIRDOSE 3 by Stabin (Fig. 1). According to these S values, ^{114m}In was obviously the best therapeutic isotope, delivering the highest dose. ^{114m}In was chosen for the human phantom study.

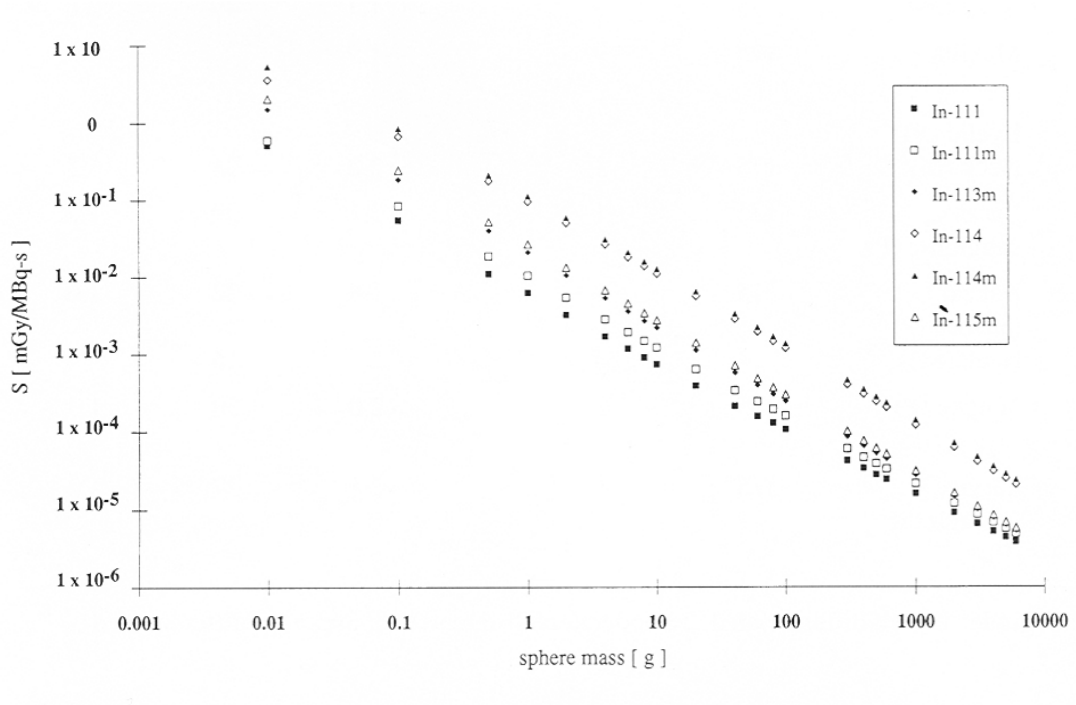

Fig. 1. Calculated S values of different isotopes of indium (^{111}In, ^{111m}In, ^{113m}In, ^{114}In, ^{114m}In, and ^{115m}In) for spherical tumors from the tabulated data in MIRDOSE 3 by Stabin (Kairemo et al. 1996b).

MIRD phantom geometry was used to obtain the S values (absorbed dose in a target organ/region per cumulated activity in a source organ/region) for ^{111}In and ^{114m}In for a realistic geometry. A slice through the MIRD phantom is given in Figure 1A of Study V. The head and the spine (solid lines) were defined in MIRD pamphlet no. 5 (Snyder et al. 1969), and the blood vessels, tumor, and metastases (broken lines) were determined using the CT

study of one of the SCC patients (#9/79/F). A coronal slice of the same geometry is shown in Figure 1B of Study V.

While tracing the photons, each location of energy depositions was verified, and if an energy deposition was made inside a predefined region (a MIRD organ or user-defined region) the absorbed energy of that region was summed. When the session was over, the S value was calculated from the absorbed energy of each region. The mass of the region and the total number of simulated decays in the source region were taken into account.

4.16. *Ex vivo* imaging using a beta camera (V)

Images with the beta camera were obtained by mounting the tissue slices on the entrance window of the beta camera. The technique is described in detail elsewhere (Ljunggren and Strand 1990). In brief, a light-sensitive detector, a multichannel detector (MCD), was equipped with a thin scintillator. When the β-particles were transferred energy to the scintillator material, light photons were created and the position of the β-particles was detected by the MCD. An image was collected by an acquisition unit and transferred to an image processing system.

4.17. Summary table

Table 5. Schematically summarized study design.

***In vitro* cell studies**	***In vivo* studies/ animals**	***In vivo* studies/ patients**
Comparison of ^{111}In-BLMC, BLM, $^{111}InCl_3$, and external beam radiation	Growth characteristics of known cell lines as xenografts	Tumor targeting, uptakes in HNSCC patients
High-dose ^{111}In-BLMC (195 MBq/mgBLM) vs. low-dose ^{111}In-BLMC (40 MBq/mgBLM)	Tumor targeting, uptakes in xenografted HNSCC	Dosimetry for HNSCC primary and metastatic tumor dosimetry for two radioisotopes
Effect of BLM and ^{111}In-BLMC on cell cycle	Therapy with ^{111}In-BLMC, BLM, and NaCl injection	

***Ex vivo* studies/ animals**	***Ex vivo* studies/patients**
Mitotic activity, proliferation, flow cytometry	Tumor targeting, tissue uptakes, beta camera imaging
	Mitotic activity, proliferation

5. Results

5.1. Cytotoxicity of BLM and external beam radiation (I)

The most significant finding was the variation in the sensitivity for BLM in different SCC cell lines, as can be seen in Table 6. Cell lines UT-SCC-19A and UT-SCC-2 differed from the others by their chemosensitivities (IC_{50} = 4.0 ± 1.3 nM, IC_{50} = 5.2 ± 0.9 nM, respectively). The most chemoresistant cell lines were UT-SCC-12A (IC_{50} = 14.2 ± 2.8 nM) and UT-SCC-9 (IC_{50} = 11.5 ± 1.1 nM). The survival curves of UT-SCC-2, UT-SCC-8, UT-SCC-9, UT-SCC-12A, and UT-SCC-19A cell lines are presented in Figure 1 (Study I).

The SF_2 values varied between 0.25 ± 0.03 for cell line UT-SCC-9 and 0.38 ± 0.02 for cell line UT-SCC-12A (Table 6). Figure 2 shows the radiation survival curves of UT-SCC-2, UT-SCC-8, UT-SCC-9, UT-SCC-12A, and UT-SCC-19A (Study I).

Table 6. ***In vitro*** **sensitivity of HNSCC cell lines to BLM and radiation in Studies I-III.**

Cell line	BLM IC_{50}±SD(nM)	^{111}In-BLMC (low) IC_{50}±SD(nM)	^{111}In-BLMC (high) IC_{50}±SD(nM)	External beam radiation SF_2±SD	External beam radiation AUC±SD(Gy)
UT-SCC-2	5.2 ± 0.9 (**I**) 6.4 ± 0.6 (**II**)	3.9 ± 0.6 (**II**)	4.2 ± 0.6 (**II**)	0.32 ± 0.05 (**I**)	1.7 ± 0.1 (**I**)
UT-SCC-8	9.4 ± 0.5 (**I**)			0.37 ± 0.03 (**I**)	1.9 ± 0.1 (**I**)
UT-SCC-9	11.5 ± 1.1 (**I**)			0.25 ± 0.03 (**I**)	1.4 ± 0.1 (**I**)
UT-SCC-12A	14.2 ± 2.8 (**I,III**) 18.8 ± 3.3 (**II**)	10.7 ± 1.8 (**II**)	12.7 ± 1.7 (**II**)	0.38 ± 0.02 (**I**)	2.1 ± 0.1 (**I**)
UT-SCC-12B	13.0 ± 1.1 (**III**)				
UT-SCC-19A	4.0 ± 1.3 (**I,III**) 4.1 ± 1.8 (**II**)	2.0 ± 0.9 (**II**)	2.6 ± 1.5 (**II**)	0.33 ± 0.03 (**I**)	1.7 ± 0.1 (**I**)

IC_{50}, Bleomycin concentration causing 50% inhibition of clonogenic cell survival.

SF_2, Survival fraction after a single radiation dose of 2 Gy.

AUC, Area under the survival curve

5.2. Cytotoxicity of BLM, ^{111}In-BLMC, and $^{111}InCl_3$ in SCC cell lines (II)

The IC_{50} values for BLM, ^{111}In-BLMC (low), and ^{111}In-BLMC (high) are listed in Table 6. The most chemosensitive cell line, UT-SCC-19A, had an IC_{50} value of 4.1 ± 1.8 nM. The IC_{50} value for ^{111}In-BLMC (low) was 2.0 ± 0.9 nM. ^{111}In-BLMC (high) was more effective (IC_{50} = 2.6 ± 1.5 nM) than BLM, but less effective than ^{111}In-BLMC (low). Differences are distinct also in Figure 1 (Study II).

The UT-SCC-2 cell line was chemosensitive (IC_{50} = 6.4 ± 0.6 nM). The IC_{50} values for ^{111}In-BLMC (low) and ^{111}In-BLMC (high) were 3.9 ± 0.6 nM and 4.2 ± 0.6 nM, respectively. In Study II, Figure 2 shows the survival curves of the UT-SCC-2 cell line.

The most chemoresistant cell line, UT-SCC-12A, had an IC_{50} value of 18.8 ± 3.3 nM. Experiments with this cell line also showed a cytotoxic effect of ^{111}In-BLMC (Study II, Figure 3). ^{111}In-BLMC (low) and ^{111}In-BLMC (high) had lower IC_{50} values than BLM, 10.7 ± 1.8 nM and 12.7 ± 1.7 nM, respectively.

$^{111}InCl_3$ was not cytotoxic to the three cell lines used (Study II, Figures 1-3).

In testing the IC_{50} values (N=14) of the three SCC cell lines, ^{111}In-BLMC (low) was a more effective cell killer than BLM (p = 0.0016 **). ^{111}In-BLMC (high) was also superior to BLM (p = 0.0029 **). Surprisingly, ^{111}In-BLMC (low) was more effective than ^{111}In-BLMC (high) (p = 0.0023 **).

5.3. SCC cell lines *in vitro* and *in vivo* (III)

In *in vitro* studies, IC_{20}, IC_{50}, and IC_{90} values varied between the SCC cell lines (Study III, Table II). IC_{50} values for UT-SCC-12A and UT-SCC-12B were 14.2 ± 2.8 nM and 13.0 ± 1.1 nM, respectively. IC_{20} values were similar for these two cell lines, whereas a marked difference was present in IC_{90} values, 59.6 ± 2.8 nM and 44.7 ± 1.1 nM (Study III, Table II). The most chemosensitive cell line, UT-SCC-19A had an IC_{50} value as low as 4.0 ± 1.3 nM. Cell survival data are shown in Figure 1 (Study III).

In *in vivo* studies, the tumors showed growth on the flank in five out of ten animals. Xenografted mice preserved their vitality and their mean weight increased by 2.8 ± 0.6 g within 35 days. The tumors started to grow intensively 25 days after SCC cell inoculations. The mean tumor volumes are presented as a function of time in Figure 2 (Study III), demonstrating an exponential pattern of growth. For instance, at 25 and 35 days, the tumor volumes were 111 ± 51 mm^3 and 874 ± 577 mm^3, respectively. Calculated from the fitted curve, the tumor doubling time was 3.86 ± 0.76 days.

5.4. ^{111}In-BLMC in HNSCC xenograft tumors (IV)

5.4.1. Gamma camera imaging

The tumors of the UT-SCC-12A and UT-SCC-19A cell lines are seen in Figure 2 (Study IV). Activity ratios of ^{111}In-BLMC on gamma camera images are shown in Table 1 (Study IV). The UT-SCC-19A-xenografted mouse had the highest T/non-T uptake ratio of 7.54 at 4 h after ^{111}In-BLMC injection. The first image of the UT-SCC-12A-xenografted mouse was taken at 8 h and showed a T/non-T activity ratio of 5.13. Tumor-to-whole body ratios are also provided in Table 1 (Study IV).

5.4.2. Therapeutic trial

During the 14-day trial, no mice died. The relative weight ratios (excluding that of the tumor mass), and the body weight on each examination day divided by the initial weight are plotted in Figure 3 (Study IV). The weights were 22.7-24.8 g before the first injections.

The final weight reductions, excluding that of the tumor mass, in the control group were 3.7%, 5.0%, 5.8% and 9.1%. In the BLM group, the proportions of reductions were 2.7% and 4.2%; and in the ^{111}In-BLMC group 2.0% and 4.0%.

The log(RTS) curves of mice, which received NaCl, BLM, or ^{111}In-BLMC are shown in Figure 4 (Study IV). The growth curves flattened out after exposure to BLM and ^{111}In-BLMC before re-growth 7-9 days after the first injection of the drug. Either of these two drugs was more effective than NaCl.

5.4.3. DNA flow cytometry

Histopathologically, all xenograft tumors consisted of vital carcinomatous squamous cells. Less than five mitoses per high power field (HPF) were found in tumors of the NaCl group. More than five mitoses per HPF were counted in re-growing tumors of both BLM and ^{111}InBLMC groups, as shown in Table 2 (Study IV).

The results revealed the heterogeneity of Ki-67 staining in different tumor regions. The Ki-67 immunoreactivity was scored as 2 or 3 in three tumors of the NaCl group. Immunostaining remained negative in one tumor. In both the BLM and the ^{111}In-BLMC groups, by contrast, Ki-67 nuclear-positive cells formed the majority, and tumor staining was scored as 3.

DNA analysis was performed on all tumors. The tumors showed euploidy and aneuploidy, as presented in Table 2 (Study IV). The highest flow cytometric aneuploidy values, 1.14 and 1.15, were obtained in the NaCl group. The total S phase value of the NaCl group ranged from 1.51% to 9.21%. The corresponding values for the BLM and ^{111}In-BLMC groups were 2.84% and 3.38%; 5.41% and 7.65%, respectively.

The flow cytometry of the three SCC cell lines showed aneuploidy and even tetraploidy in cell lines UT-SCC-2 and UT-SCC-19A. The DNA index (DI) of UT-SCC-19A after a one-day exposure to the diluent, BLM, or ^{111}In-BLMC was 2.03, 2.17, and 2.16, respectively. The S phase fractions (SPF) were 45.8%, 42.1%, and 30.9%. The DIs of the cell line UT-SCC-2 after the same exposure to drugs were 2.84, 2.89, and 2.90, and the SPF values 24.4%, 24.8%, and 25.7%, respectively. In contrast to the preceding, the DI value of cell line UT-SCC-12A was 1.57 in the control, BLM, and ^{111}InBLMC groups.

The cell cycle data were calculated using MultiCycle software. The proportions of G1/G0, S, and G2/M phases of three UT-SCC cell lines are shown in Tables 7 and 8. However, the proportions of the G2/M phase in cell lines UT-SCC-19A exposed to diluent, BLM, and ^{111}In-BLMC were 16.1%, 26.8%, and 49.6%, respectively. After two days of exposure to drugs, the DNA histogram profile was similar to that after one day of exposure, as shown in Figure 5 (Study IV).

Table 7. Cell cycle data after 24-h exposure to diluent, BLM, or ^{111}In-BLMC.

Cell line		G1/G0 phase (%)	G2/M phase (%)	S phase (%)
UT-SCC-2	diluent	51.7	25.3	23.0
UT-SCC-2	BLM	45.7	30.5	23.8
UT-SCC-2	^{111}In-BLMC	43.3	31.4	25.3
UT-SCC-12A	diluent	41.9	22.7	35.4
UT-SCC-12A	BLM	40.6	24.2	35.2
UT-SCC-12A	^{111}In-BLMC	39.5	27.4	33.1
UT-SCC-19A	diluent	37.7	16.1	46.2
UT-SCC-19A	BLM	31.2	26.8	41.9
UT-SCC-19A	^{111}In-BLMC	17.9	49.6	32.5

Table 8. Cell cycle data after 48-h exposure to diluent, BLM, or ^{111}In-BLMC.

Cell line		G1/G0 phase (%)	G2/M phase (%)	S phase (%)
UT-SCC-2	diluent	73.6	11.4	15.1
UT-SCC-2	BLM	70.3	14.5	15.2
UT-SCC-2	^{111}In-BLMC	60.7	19.8	19.6
UT-SCC-12A	diluent	50.8	20.8	28.4
UT-SCC-12A	BLM	50.4	20.8	28.8
UT-SCC-12A	^{111}In-BLMC	49.0	23.1	27.9
UT-SCC-19A	diluent	47.6	11.0	41.4
UT-SCC-19A	BLM	41.7	15.8	42.5
UT-SCC-19A	^{111}In-BLMC	26.7	37.9	35.4

5.5. Biokinetics of ^{111}In-BLMC implementations for radiochemotherapy (V)

Tumor characteristics and uptake of ^{111}In-BLMC are shown in Table I (Study V). The uptake was measured as a region of interest (ROI) ratio between tumors and nontumors, cor-

responding to the location on the contralateral side, from planar gamma camera images. The ratio varied from 1.2 to 2.8 in malignant tumors, and was 1.0 in one benign tumor (#7/58/F). The uptake of ^{111}In-BLMC was unaffected by the fivefold increase in injected radioactivity dose. The tumor grades, frequency of mitoses, and proliferation grades were in close correlation with each other, varying between 1 and 3 in malignant tumors and were all graded 0 in benign tumors (Table 9). Moreover, an evident correlation existed between grade and uptake of ^{111}In-BLMC (correlation coefficient R = 0.566).

The effective half-life,

$$T_{1/2,eff} = (t_{1/2,phys} \cdot t_{1/2,biol}) / (t_{1/2,phys} + t_{1/2,biol}) \quad (2)$$

where $t_{1/2,,phys}$ and $t_{1/2,biol}$ are the physical and biological half-lives, for radioactivity was 1.5-3.1 h in serum and 1.4-3.7 h in urine. About half of the activity was excreted in urine within 3 h, and more than 95% within 22 h. Tumor sample uptakes varied between 0.1 and 0.95 x 10^{-3}% of injected dose (ID/g at 48 h) in malignant tumors. In benign fibroma, the uptake was 0.06 x 10^{-3}% of injected dose (ID/g at 48 h). Measured absolute uptakes in tumor samples correlated with ^{111}In-BLMC uptake on images (R = 0.705). The uptake of ^{111}In-BLMC, measured from tumor samples, correlated with the frequency of mitoses (R = 0.734) and the grade of proliferation (R = 0.846). The effective half-life for tumor tissue varied from 16 to 49 h.

S values were obtained for the regions and organs of interest in images (Study V, Table II). Tumor (user-defined), metastasis (user-defined), total body, kidneys, and liver were used as source organs/regions when tumor dose was calculated from the computed tomographic (CT) and SPET data for one SCC patient (#9/79/F). The thyroid was considered a target organ. MIRD pamphlet no.11 published S values, which were converted into Gy/MBqh, are presented in Table II (Study V). Our simulated S values for ^{111}In and ^{114m}In and the ratios of S values for ^{114m}In to ^{111}In are shown in the same table. For example, the calculated S value for internal tumor dose ($Tumor_{source} \rightarrow Tumor_{target}$) was 2.04x$10^{-3}$ Gy/MBqh for patient #9/79/F (Study V, Table II).

The physical half-life differs between the two radionuclides (2.8 days for ^{111}In and 49.5 days for ^{114m}In). Thus, the effective half-lives differ widely, assuming the same biological half-life.

The ratio (^{114m}In /^{111}In) of the effective half-lives is 1.6 when the biological half-life is 2 days. The ratio becomes 3.8 with a biological half-life of 10 days.

In the kidneys, the dosimetric estimate for a 3700 MBq dose was 2.2 Gy (tolerance 20 Gy), when the mean residence time (MRT), determined from the imaging data, was 5 h. When assuming an MRT of 16 h in a 14-g tumor (MIRD formalism), the tumor dose was 0.66 cGy/MBq. Patient #9/79/F had a tumor of this size, and MRT in this case corresponds to the shortest half-life observed in the tumor.

The SCC tissue slices, containing approximately ^{111}In-BLMC 1 kBq/g, were imaged with a beta camera for 6-8 h. The activity at 48 h was distinctly concentrated in the malignant tumor (yellow areas), representing an SCC of the tongue base (Study V, Figure 2A). In Figure 2B, which represents a low-grade mesenchymal malignant tumor, the overall activity was significantly lower than in Figure 2A (Study V, Figure 2B). Heterogeneous uptakes in tissue slices can be observed in beta camera images also within the tumor.

Table 9. Patient data.

	Injected activity 75 MBq (4 patients)	**Injected activity 175 MB** (3 patients)	**Injected activity 375 MBq** (3 patients)
Blood $T_{1/2}$ (h)	1.5 – 1.9	1.9 – 3.1	1.8 – 2.1
Tumor $T_{1/2}$ (h)	20 – 49	29 – 34	16 – 30
Absolute tumor uptake (%ID/g x10^{-3})	0.11 – 0.95	0.06 – 0.58	0.22 – 0.9
Tumor uptake	1.4 – 2.8	1.0 – 1.5	1.2 – 1.6
Mitoses	2; 2; 3; 3; 3; 3	0; 3; 1	1; 3; 3; 2
Ki-67 staining	2; 1; 2; 3; 3; 3	0; 2; 1	1; 3; 3; 3
Grade	2; 2; 3; 3; 3; 3	0; 3; 1	1; 3; 3; 3

6. Discussion

Head and neck squamous cell carcinoma is the sixth most common cancer in the world, and approximately two-thirds of HNSCCs are in stage III/IV at presentation. In Finland, HNSCCs represent 2.6% of all new malignancies (Finnish Cancer Registry 2006). Despite combined modality therapies, including surgery, external radiation, and chemotherapy, the 5-year overall survival rate of stage III and IV disease remains at 40%. Novel approaches such as nuclear medicine, are needed to improve patient outcome.

In this thesis, we have studied the usefulness of ^{111}In-BLMC in the diagnostics and therapy of HNSCC using *in vitro* HNSCC cell lines and *in vivo* nude mice and also (human) HNSCC patients.

6.1. Cytotoxicity of BLM, external beam radiation, ^{111}In-BLMC, and $^{111}InCl_3$ in HNSCC cell lines *in vitro* (I-IV)

The 96-well plate clonogenic assay is a suitable method for studying HNSCC cell lines, as has been shown in several reports (Grénman et al. 1988a, Pekkola-Heino et al. 1989, Grénman et al. 1989, Pekkola-Heino et al. 1992a, Erjala et al. 2006). The cell culture based on limited dilutions reveals living cell colonies well. Up to 10-fold PE values have been observed with this method, as compared with soft agar methods. In our study, the plating efficiencies varied from 0.1 to 0.55. The most chemosensitive cell line, UT-SCC-19A, had the lowest plating efficiency. However, plating efficiency had no impact on cytotoxicity.

Studies I and III

In the literature, the sensitivity for BLM differs considerably between cell lines, from 5- to 10-fold (Urade et al. 1992). Studies have also indicated variation in inherent radiation sensitivity (Weichselbaum 1986, Grénman et al. 1988b, Pekkola-Heino et al. 1989).

Study I and the *in vitro* part of Study III confirmed earlier results of variation in SCC cell lines with respect to sensitivity for BLM (Table 6). In Study III, we used two HNSCC cell lines (UT-SCC-12A and UT-SCC-12B) that originated from a primary tumor and metasta-

sis of the same patient. The cell line UT-SCC-12B from the metastasis had an IC_{50} value of 13.0 ± 1.1 nM. The UT-SCC-12A of the primary tumor had an IC_{50} value of 14.2 ± 2.8 nM.

In Study I, differences in the IC_{50} values for BLM and the SF_2 values for irradiation between the most sensitive and resistant SCC cell lines were 3.6- and 1.7-fold, respectively. UT-SCC-12A with a high IC_{50} value for BLM (IC_{50} = 14.2 ± 2.8 nM) also had a high SF_2 value for radiation (SF_2 = 0.38 ± 0.02). The most chemosensitive cell line, UT-SCC-19A (IC_{50} = 4.0 ± 1.3 nM), had an SF_2 value of 0.32 ± 0.03. The UT-SCC-9 cell line had an IC_{50} value of 11.5 ± 1.1 nM for BLM, but had the highest sensitivity for radiation (SF_2 = 0.25 ± 0.03). This may indicate that the mechanisms for radio- and chemoresistance are at least partially different. More than one mechanism is generally likely to be responsibible for the resistance. BLM hydrolase converts BLM to an inactive desamino form, probably explaining the primary mechanism of BLM resistance (Lazo et al. 1982). Another mechanism may be elevated DNA repair activity (Iqbal et al. 1976, Dar and Jorgensen 1995).

External beam radiation has extensively been combined with DNA-active chemotherapeutics in the treatment of head and neck cancer. The rationale has been to get a benefit from the combination with the hope of a positive interaction, based on a similarity in the mechanism of action for each separate agent. An additive effect of carboplatin and radiation, paclitaxel and radiation, and vinorelbine and radiation has been reported (Pekkola-Heino et al. 1992b, Pulkkinen et al. 1996, Erjala et al. 2004).

Study I was initiated to investigate the chemo- and radiosensitive elements separately *in vitro*. The results showed that HNSCC cells respond to both BLM and external beam radiation. Our data provide a good basis for further *in vitro* and *in vivo* experiments to characterize the interaction of simultaneous radiation and BLM *in vitro*.

Study II

Concurrent chemoradiotherapy has proven more effective than neoadjuvant and adjuvant schedules in improving patient outcome (Pignon et al. 2000, Bernier and Bentzen 2002, Bourhis et al. 2007, Pignon et al. 2007). Two independent, large-scale prospective randomized trials demonstrated that simultaneous cisplatin and irradiation were more effective in control of locoregional disease and yielded longer disease-free survival than radiotherapy alone (Bernier et al. 2004, Cooper et al. 2004). This suggests that combining the radionuclide with a chemotherapeutic agent has the potential to improve patient outcome. Chemotherapeutic agents are likely to inhibit the repair of lethal and sublethal damage caused by radiation. They probably also radiosensitize hypoxic cells and synchronize tumor cells into the G2/M phase, which is the most radiosensitive phase of the cell cycle (Bernier and Cooper 2005).

BLM has been reported to function as a radiosensitizer in benign and malignant tumors (Orford et al. 1995, Sung et al. 1995). In a trial by Smid et al. (2003), locoregional control at 2 years was 69% in postoperative radiotherapy alone compared with 86% in radiotherapy combined simultaneously with mitomycin C and BLM.

Radiation affects cells at the DNA level, resulting in cell cycle disturbances and arrest in the G_2 phase, which diminishes cell divisions. Furthermore, BLM is known to be active at the DNA level, causing single- and double-strand breaks. Even-Sapir et al. (1994) have demonstrated that the uptake of ^{57}Co-BLM predicts the outcome of lung cancer patients. They found that patients with lung cancers, with a high uptake of ^{57}Co-BLM bound into the DNA after injection responded poorly to chemotherapy and had a shorter survival than patients with tumors showing lower uptake. BLM complexes are conceivable for therapy because of unexpectedly good targeting characteristics. We found a good sensitivity (93%) and specificity (100%) in the diagnostic staging of 13 head and neck cancer patients using a low-pH ^{111}In-BLMC (Kairemo et al. 1994). ^{111}In is a gamma-emitter with an energy of two gammas (171 keV and 245 keV), but it also emits Auger-electrons suitable for therapeutic purposes.

Study II clearly demonstrated that ^{111}In-BLMC (low) was more toxic to HNSCC cells than BLM in all three cell lines tested (Table 6; Study II, Figures 1-3). For UT-SCC-2, UT-SCC-12A, and UT-SCC-19A, the IC_{50} ratios between BLM and ^{111}In-BLMC (low) were 1.6-fold, 1.8-fold, and 2.1-fold, respectively. The differences between BLM and ^{111}In-BLMC (high) in the above-mentioned cell lines were 1.5- to 1.6-fold, ^{111}In-BLMC (high) being more toxic. ^{111}In activity (40 MBq/mg BLM) was more effective in killing cells than ^{111}In activity (195MBq/mg BLM). An almost fivefold increment of ^{111}In activity of the complex did not increased cytotoxicity. Clinically, specific activities of 40-100 MBq/mg BLM have been used. Higher ^{111}In activities, such as 195 MBq/mg BLM, have not been used in patients. Obviously, the relative biological effectiveness (RBE) of Auger-electrons is high using ^{111}In-BLMC (low). This may mean, that when the saturation concentration is reached, the addition of ^{111}In activity will not increase cytotoxicity. Higher radioactivity doses may damage the properties of BLM. Superfluous labeling might cause radiolysis, with a similar effect as immunoreactivity in labeling of antibodies.

In vitro and *in vivo* experiments with Auger-emitter ^{111}In, which was localized in the cell nucleus via the radiochemical ^{111}In-oxine, but did not bind to DNA, produced an RBE value of ~ 4 (Rao et al. 1988, McLean et al. 1989). RBE has been shown to be 7-9 for ^{125}I, whereas it is considered to be 1 for external beam radiation (Howell et al. 1993, Narra et al. 1994). In addition to the nature and energy of the radiation, the effectiveness of producing biological damage via radionuclides depends on biokinetics and subcellular distribution. Auger-electrons deliver their energy, $10^4 – 10^7$ Gy/decay, within a radius of one nanometer to 0.5 μm around the decay site (Kassis and Adelstein 2005). Faraggi et al. (1994) demonstrated that the absorbed dose rate at the center of the cell is 18 times higher if radioactivity of ^{111}In is localized within the cell nucleus than if it is situated on the cell membrane. The close proximity of the Auger-electron-decaying atom to DNA leads to high-LET-type radiation effects. This has been confirmed by *in vitro* studies; the Auger-emitter bound to nuclear DNA has caused a monoexponential decrease in survival (Kassis et al. 1987b), while decay within the cytoplasm or extracellularly has produced survival curves typical of x-rays (Kassis et al. 1987a).

$^{111}InCl_3$ was not cytotoxic in this study. Hou et al. (1989a) demonstrated a corresponding result with human small cell lung cancer cells.

^{111}In-BLMC, which has a tumor-seeking and DNA-splitting nature, has an *in vitro* synergy compared with BLM.

Study IV

BLM is known to be active at the DNA level, causing single- and double-strand breaks (Iqbal et al. 1976, Kohn and Ewig 1976, Cheong and Iliakis 1997). Some investigators have reported an ability of BLM to block cells reversibly in the G_2 phase (Barranco et al. 1973b, Constanzi et al. 1976). However, BLM is not generally considered to induce alterations in the cell cycle, as is the case with paclitaxel. Paclitaxel clearly produced a G2/M block in the cell cycle of cell line UT-SCC-19A (Elomaa et al. 1995).

The flow cytometric results of the three UT-SCC cell lines used were interesting. In all cell lines, the percentage of cells in the G2/M phase increased after exposure to BLM, especially ^{111}In-BLMC (Tables 7 and 8). In Study I, cell line UT-SCC-19A was more sensitive to BLM and external radiation than cell lines UT-SCC-2 and UT-SCC-12A. In Study IV, the proportion of UT-SCC-19A cells in the G2/M phase was 16.1%, 26.8%, and 49.6% in the control, BLM, and ^{111}In-BLMC groups, respectively (Study IV, Figure 5). By contrast, the proportion of cells in the G0/G1 phase appeared to diminish from 37.7% in the control group to 31.2% in the BLM group and 17.9% in the ^{111}In-BLMC group. A corresponding tendency was seen with the UT-SCC-2 and UT-SCC-12A cell lines.
Our results suggest that BLM and particularly ^{111}In-BLMC seem to induce alterations in the cell cycle by producing a G2/M block. The G2/M phase of the tumor cell cycle is the most sensitive to irradiation (Sinclair 1968). In a flow cytometric study, Sham and Durand (1999) observed a radiation-induced G2 block after external beam radiation of human cervical SCC xenograft tumors in SCID mice.

6.2. ^{111}In-BLMC in SCC xenograft tumors (III, IV)

An urgent need exists to develop strategies for the diagnostics and treatment of HNSCC.
Genetic engineering in mouse models for HNSCC has recently progressed (Lu et al. 2006). Experimental mouse models recapitulate the growth of human HNSCCs. For example,

comparison of the effect between different therapies yields important information, although these results are not directly applicable in the clinic.

Study III

Xenografted mouse experiments are sensitive to disturbances. Thus, a 50% tumor growth in the flank was acceptable in Study III. Between days 25 and 35, growth of the tumors was rapid, the doubling time being 3.9 days. This result gave a good basis for further tumor xenograft experiments in Study IV, particularly for dose planning in treatment with ^{111}In-BLMC.

In subsequent studies, cytotoxicity might be increased using Auger-emitting BLMC in combination with electrochemotherapy (ECT). ECT is an antitumor approach that combines systemic BLM with electric pulses (EPs) delivered locally at the tumor site. EPs increase the permeability of the cell membrane in the tissue, allowing BLM delivery inside the cells, probably also increasing the cytotoxicity of ^{111}In-BLMC (Domenge et al. 1996).

Study IV

In the imaging study, xenografted tumors of cell lines UT-SCC-12A and UT-SCC-19A were observed in planar images (Study IV, Figure 2). Hou et al. (1984a, 1984b) demonstrated ^{111}In-BLMC affinity to viable tumors in glioma-bearing mice.

In the therapeutic study, after the weight loss correction, the final loss in the two cell lines turned out to be 2.7% and 4.2% in the BLM group and 2.0% and 4.0% in the^{111}In-BLMC group (Study IV, Figure 3). Thus, a 15% weight loss, which is usually considered a significant indicator for maximum tolerated dose in preclinical radionuclide therapy trials, was not achieved. Tumors receiving BLM and ^{111}In-BLMC showed a flattening of their growth curves, whereas control tumors reached exponential growth (Study IV, Figure 4). In addition, seven of eight tumors showed regrowth at the time animals were sacrificed. Sham and Durand (1999) investigated cell kinetics and repopulation parameters of xenografts in SCID mice using continuous or split course external irradiation. The regrowth rate of these tumors matched that of untreated tumors after regression, which followed the split course irradiation.

Based on Ki-67 antigen activity and number of mitoses, the proliferative activity was stronger in the BLM and ^{111}InBLMC groups than in the NaCl group, indicating regrowth of the tumors (Study IV, Table 2). Heterogeneity in Ki-67 staining was observed. Variation in proliferation and cellular differentiation in different tumor regions of HNSCC has been shown (Jacob et al. 1996). Flow cytometry expressed a slight difference in ploidy status, which was not typical of any given therapy group.

The beneficial effect of BLM has consistently been demonstrated in experiments using xenografted HNSCCs (Wahlberg et al.1987, Elprana et al. 1992). Radioactive (^{191}Pt) cis-platin has been shown to be more effective than cisplatin alone in decreasing tumor size in nude mice (Areberg et al. 2001). The efficacy of a ^{186}Re-labeled monoclonal antibody has been shawn in HNSCC and ovarian cancer xenografts, this antibody can be used to cause a total ablation of these tumors (Gerretsen et al. 1993, Kievit et al. 1997).

Some *in vivo* therapy studies with DNA-incorporated Auger-electron-emitting radionuclides have demonstrated excellent results in (Baranowska-Kortylewicz et al. 1991). A 5-log reduction in intraperitoneal ascites ovarian cancer cell survival has been observed in mice treated with ^{125}I-UdR (Bloomer and Adelstein 1977). In another therapy study, rats with intrathecal tumors received therapeutic doses of ^{125}I-UdR intrathecally and in addition to methotrexate; 5- to 6-log tumor cell reduction and 30% improvement in tumor-bearing rats was shown (Kassis et al. 2004).

In this study, BLM and ^{111}In-BLMC were more effective than NaCl in reducing tumor size in HNSCC (Study IV, Figure 4). Hou et al. (1985) tested ^{111}In-BLMC therapy in glioma-bearing mice and found ^{111}In-BLMC to be superior to BLM in reducing tumor size.

However, a thorough comparison between the BLM and ^{111}In-BLMC groups in this study could not be conducted due to the small number of mice. Our findings should, however, provide impetus for further experiments concerning therapeutic applications using more animals and possibly with more radio- and chemosensitive cell lines. Dose and schedule of drug administration are important elements in fine-tuning future therapeutic applications.

6.3. Clinical experiments: biokinetics of ^{111}In-BLMC implementations for radiochemotherapy (V)

Study V

This study confirms the tumor-seeking behavior of ^{111}In-BLMC in HNSCC (Table 9; Study V, Table I) shown in our previous patient study (Kairemo et al. 1996b). Table 9 clearly demonstrates that uptake of ^{111}In-BLMC was unaffected by a fivefold increment in injected radioactivity. A set level of uptake was achieved with the lower doses. In the patient study, the specific activity of the complex was the same, 100 MBq/mg BLM. In the *in vitro* study there were two specific activities, 40 MBq/mg BLM and 195MBq/mg BLM, of the complex. Interestingly, an almost fivefold increment of ^{111}In activity did not increase cytotoxicity.

Using diagnostic doses of ^{111}In-BLMC (75-375 MBq), no side-effects were seen in head and neck cancer patients. The uptake ratio received from gamma images varied from 1.2 to 2.8 in malignant tumors, and was 1.0 in the benign tumor. Under certain conditions, it might be possible to distinguish benign disease from malignant disease. An obvious correlation existed between the grade and the uptake of ^{111}In-BLMC (Table 9). Even-Sapir et al. (1994) demonstrated that the uptake of ^{57}Co-BLM predicts the outcome of lung cancer patients. They found that patients with lung cancer tumors who had a high uptake of ^{57}Co-BLM responded poorly to chemotherapy and had a shorter survival time than patients with tumors showing a lower uptake.

The tumor grade, frequency of mitoses, and proliferation grade, measured using MIB immunohistochemistry, were in close correlation with each other and varied between 1 and 3 in malignant tumors, and were all graded 0 in the benign tumor (Table 9). Malignant tumors with strong proliferation activity and poor prognosis might have higher uptake of the radiochemotherapeutic agent. This information could be useful in therapy planning.

The effective half-lives for radioactivity in serum and urine are consistent with the results of others (Crooke et al. 1977, Kramer et al. 1978). Labeling of BLM did not essentially change the serum half-life or the plasma clearance rate. The effective half-life for the tu-

mor tissue varied between 16 and 49 h. This shows an overall rapid clearance rate from normal organs and slower clearance from targeted tumor tissue.

Heterogeneous uptake of ^{111}InBLMC within the tumor and between the tumors was observed in beta camera images (Study V, Figures 2A and 2B).

The kidneys were considered to be a critical organ. The estimate for a 3700 MBq dose, assuming a mean residence time (MRT) of 5 h (blood), was 2.2 Gy, which is under the tolerance dose of 20 Gy. The tumor dose was 0.66 cGy/MBq, when assuming a MRT of 16 h, in a 14-g tumor (MIRD formalism). In this case, the total tumor dose would be 24.4 Gy, corresponding to the tumor size of patient #9/79/F. MRT in this case was similar to the shortest half-life observed in tumor samples.

Radionuclide-based therapy requires a suitable carrier, appropriate physical properties of the radionuclide, and knowledge of the interaction between the radionuclide-based agent and its biological environment. Theoretically, substituting ^{111}In with ^{114m}In might lead to a better cytotoxic effect because of the higher energy of Auger-electrons and a longer half-life of 49.5 days. Regarding the S values for ^{111}In and ^{114m}In, i.e. the absorbed dose in a target region per cumulated activity in the source organ, ^{114m}In seems to give higher absorbed doses at short ranges. We simulated S values for ^{111}In and ^{114m}In, and with ratios of S values for ^{114m}In to ^{111}In, in Gy/MBqhs. The calculated ratio of the S values for ^{114m}In to ^{111}In ($\text{Tumor}_{\text{source}} \rightarrow \text{Tumor}_{\text{target}}$) was 16.127 (Study V, Table II). The ratio of the S values for ^{114m}In to ^{111}In ($\text{Total body}_{\text{source}} \rightarrow \text{Total body}_{\text{target}}$) was 4.135. Thus, $[\text{S(Tumor)/S(Total body)}]^{\text{In-114m}}/[\text{S(Tumor)/S(Total body)}]^{\text{In-111}}$ was approximately 4.

Rapid advances are being made in the field of targeted radionuclide therapy. Auger-electron emitters, e.g. ^{111}In and ^{114m}In, represent an attractive alternative in the treatment of advanced HNSCC. The possibility exists of finding even more effective carriers, such as nanoparticles, which would bring the Auger-emitters in very close proximity to DNA.

7. Conclusions

In this thesis, *in vitro* and *in vivo* suitability of the Auger-emitter ^{111}In-labeled BLM for diagnosis and potential therapy of HNSCC was demonstrated as follows:

1. The response of HNSCC cells to BLM and external beam radiation *in vitro* was demonstrated. We also found variation in the sensitivity for BLM and external beam radiation in different HNSCC cell lines. One cell line was sensitive to radiation, but not to BLM.

2. The Auger-emitting ^{111}In-BLMC was more toxic than BLM in all three tested HNSCC cell lines, indicating the synergistic nature of ^{111}In-BLMC.
$^{111}InCl_3$ alone was not cytotoxic.

3. ^{111}In activity of 40 MBq/mg BLM was more effective in killing cells than ^{111}In activity of 195MBq/mg BLM. An almost fivefold increment of ^{111}In activity did not increase cytotoxicity. In fact, the increase of ^{111}In activity in ^{111}In-BLMC weakened the cytotoxic effect.

4. In all cell lines, the percentages of cells in the G2/M phase increased after exposure to BLM, especially to ^{111}In-BLMC. BLM and particularly ^{111}In-BLMC seemed to induce alterations in the cell cycle by producing a G2/M block.

5. The activity ratios of ^{111}In-BLMC expressed tumor-seeking behavior in UT-SCC-12A and UT-SCC-19A xenografted mice. The xenograft tumors of cell lines UT-SCC-12A and UT-SCC-19A were also observed in planar images.

6. Tumors receiving BLM and ^{111}In-BLMC showed a flattening of their growth curves, indicating the cytotoxic effect of the drugs, whereas control tumors reached exponential growth. However, a thorough comparison between BLM and ^{111}In-BLMC groups was not possible due to the small number of mice.

7. The uptake ratios revealed by gamma images indicated tumor-seeking behavior of ^{111}In-BLMC. Measured absolute uptakes in tumor samples correlated with ^{111}In-BLMC uptakes on images. The uptake of ^{111}In-BLMC was unaffected by a fivefold increment in injected radioactivity. A positive correlation existed between ^{111}In-BLMC uptake, Ki-67/MIB activity, and number of mitoses.

8. Judging from the S values for ^{111}In and ^{114m}In, which indicate the absorbed dose in a target region per cumulated activity in a source organ, ^{114m}In seemed to give higher absorbed doses at short ranges, and thus, cytotoxicity might be more effective with ^{114m}In-BLMC than with ^{111}In-BLMC at the DNA level.

Acknowledgments

This study was carried out at the Departments of Otorhinolaryngology – Head and Neck Surgery of Helsinki and Turku University Hospitals and Universities, Finland, in cooperation with the Department of Medical Biochemistry of the University of Turku, Finland, and the Departments of Clinical Chemistry, Oncology, and Pathology of Helsinki University Hospital, Finland.

This work was financially supported by the Research Funds of the Helsinki University Hospital and Turku University Hospital, the Finnish Research Foundation of Otology, and the Finnish Foundation for Cancer Research.

I am grateful to Professor Anne Pitkäranta, Professor Jukka Finne, Professor Heikki Joensuu, and Docent Hans Ramsay for providing excellent working facilities at their departments.

My warmest appreciation is due to my supervisors Docent Kalevi Kairemo, Professor Reidar Grénman, and Docent Hans Ramsay. Kalevi suggested the subject of this thesis and guided me enthusiastically with new ideas in the exciting field of Nuclear Medicine. He always found time to discuss the many questions I had over the years. Reidar introduced me to the fascinating field of cell culturing in Turku. His passionate approach to research, logical thinking, and excellent guidance in manuscript writing were instrumental in my completing this project. Hans´ assistance was invaluable in both my scientific and clinical work at the Department of Otorhinolaryngology – Head and Neck Surgery of the University of Helsinki. His encouragement is deeply appreciated.

My sincere thanks are owed to Professor Matti Anniko and Docent Tapani Lahtinen, official referees appointed by the Medical Faculty of the University of Helsinki, for valuable suggestions, that greatly improved this manuscript. Docent Tapani Lahtinen´s background as a physicist with a long experience in radiation physics has been invaluable to me during the writing of the summary and 1´m deeply grateful for the many fruitful discussions and the time he has given me.

I am grateful to Docent Jarmo Kulmala for advice in mathematical analyses and in external beam radiation in *in vitro* experiments.

Professor Timo Paavonen and Docent Jussi Tarkkanen are thanked for assistance in histopathological, immunohistochemical, and flow cytometry work. I am also grateful to Kirsi Pekkola-Heino, Md, PhD, and Tapani Korppi-Tommola, LicPhil, for collaboration in Studies I and IV, respectively.

My author-editor Carol Ann Pelli, HonBSc, is thanked for reviewing the English language of this manuscript.

I thank Marita Potila for skillful guidance in cell culturing.

My friends, relatives, and coauthors are warmly acknowledged for their friendship over these trying years.

My heartfelt thanks are owed to my parents Aili and Paavo Jääskelä for providing unfailing love and support at all times.

I owe my deepest gratitude to my husband Docent Arto Saari, DSc (Eng), for all kinds of practical help and encouragement. His supportive and loving nature, which has been refined over the years in the raising of our four sons, has been invaluable to our family life as well as to my research. Finally, I thank my children Esko (11), Eljas (6), Alvar (6), and Samuel (3) for all the happiness that they have brought into my life.

References

Adelstein DJ, Lavertu P, Saxton JP, Secic M, Wood BG, Wanamaker JR, Eliachar I, Strome M, Larto MA. Mature results of a phase III randomized trial comparing concurrent chemoradiotherapy with radiation therapy alone in patients with stage III and IV squamous cell carcinoma of the head and neck. Cancer 88:876-883, 2000.

Ahonen A, Savolainen S, Bergström K. Isotooppilääketieteen menetelmien perusteet. In the Kliininen fysiologia ja isotooppilääketiede, First Edition. Edit. Sovijärvi A, Ahonen A, Hartiala J, Länsimies E, Savolainen S, Turjanmaa V, Vanninen E. Kustannus OY Duodecim, Helsinki 2003: 23-29.

Aisner J, Jacobs M, Sinabaldi V, Gray W, Eisenberger M. Chemoradiotherapy for the treatment of regionally advanced head and neck cancers. Semin Oncol 21(5 Suppl 12):35s-54s, 1994.

Alanen KA, Klemi PJ, Taimela S, Joensuu H. A simple preservative for flow cytometric DNA analysis. Cytometry 10(1):86-89, 1989.

Alberts DS, Chen HSG, Liu R, Himmelstein KJ, Mayersohn M, Perrier D, Gross J, Moon T, Broughton A, Salmon SE. Bleomycin pharmacokinetics in man. I. Intravenous administration. Cancer Chemother Pharmacol 1:177-181, 1978.

Ang KK. Altered fractionation in the management of head and neck cancer. Int J Radiat Biol 73(4):395-399, 1998.

Areberg J, Wenneberg J, Johnsson A, Norrgren K, Mattsson S. Antitumor effect of radioactive cisplatin (^{191}Pt) on nude mice. Int J Radiat Oncol Biol Phys 49(3):827-832, 2001.

Ariyan S. The pectoralis major myocutaneous flap. A versatile flap for reconstruction in the head and neck. Plast Reconcstr Surg 63:73-81, 1979.

Arrighi JA, Dilsizian V. Assessment of myocardial viability by radionuclide and echocardiographic techniques: is it simply a sensitivity and specificity issue? Curr Opin Cardiol 21:450-456, 2006.

Baranowska-Kortylewicz J, Makrigiorgos GM, Van den Abbeele AD, Berman RM, Adelstein SJ, Kassis AI. 5-[^{123}I]iodo-2′-deoxyuridine in the radiotherapy of an early ascites tumor model. Int J Radiat Oncol Biol Phys 21:1541-1551, 1991.

Barlogie B, Drewinko B, Schumann J, Freireich EJ. Pulse cytophotometric analysis of cell cycle perturbation with bleomycin in vitro. Cancer Res 36:1182-1187, 1976.

Barranco SC, Humphrey RM. The effects of bleomycin on survival and cell progression in Chinese hamster cells in vitro. Cancer Res 31:1218-1223, 1971.

Barranco SC, Luce JK, Romsdahl MM, Humphrey RM. Bleomycin as a possible synchronizing agent for human tumor cells in vivo. Cancer Res 33:882-887, 1973a.

Barranco SC, Novak JK, Humphrey RM. Response of mammalian cells following treatment with bleomycin and 1,3-Bis(2-chloroethyl)-1-nitrosurea during plateau phase. Cancer Res 33:691-694, 1973b.

Bentzen SM, Dische S. Late morbidity: the Damocles Sword of radiotherapy? Radiother Oncol 61:219-221, 2001.

Bernier J, Bentzen SM. Altered fractionation and combined radio-chemotherapy approaches: pioneering new opportunities in head and neck oncology. Eur J Cancer 39:560-571, 2003.

Bernier J, Domenge C, Ozsahin M, Matuszewska K, Lefébvre J-L, Greiner RH, Giralt J, Maingon P, Rolland F, Bolla M, Cognetti F, Bourhis J, Kirkpatrick A, van Glabbeke M. Postoperative irradiation with or without concomitant chemotherapy for locally advanced head and neck cancer. N Engl J Med 350:1945-1952, 2004.

Bernier J, Cooper JS. Chemoradiation after surgery for high.risk head and neck cancer patients: How strong is the evidence? Oncologist 10:215-224, 2005.

Bethge WA, Sandmaier BM. Tageted cancer therapy using radiolabeled monoclonal antibodies. Technology in Cancer Research Treatment 4(4):393-405, 2005.

Bloomer WD, Adelstein SJ. 5-^{123}I-iododeoxyuridine as prototype for radionuclide therapy with Auger emitters. Nature 265:620-621, 1977.

Blot WJ. Alcohol and cancer. Cancer Res 52 (7):2119s-2123s, 1992.

Bodei L, Kassis AI, Adelstein SJ, Mariani G. Radionuclide therapy with Iodine-125 and other Auger-electron-emitting radionuclides: Experimental models and clinical applications. Cancer Biother Radiopharm 18(6):861-877, 2003.

Bourhis J, Eschwege F. Radiotherapy-chemotherapy combinations in head and neck squamous cell carcinoma: overview of randomized trials. Anticancer Res 16:2397-2402, 1996.

Bourhis J, Galais G, Lapeyre M, Tortochaux J, Alfonsi M, Sire C, Bardet E, Rives M, Bergerot P, Rhein B, Desprez B. Concomitant radiochemotherapy or accelerated radiochemotherapy: analysis of two randomized trials of the french head and neck cancer group (GORTEC). Semin Oncol 31:822-826, 2004.

Bourhis J, Le Maître A, Baujat B, Audry H, Pignon J-P. Individual patients' data meta-analyses in head and neck cancer. Curr Opin Oncol 19:188-194, 2007.

Buchsbaum DJ. Imaging and therapy of tumors induced to express somatostatin receptor by gene transfer using radiolabeled peptides and single chain antibody constructs. Semin Nucl Med 34:32-46, 2004.

Buchsbaum DJ, Chaudhuri TR, Zinn KR. Radiotargeted gene therapy. J Nucl Med 46:179s-186s, 2005.

Burger RM, Peisach J, Horwitz SB. Mechanisms of bleomycin action: *in vitro* studies. Life Sci 28:715-727, 1981.

Börjesson PKE, Postema EJ, Roos JC, Colnot DR, Marres HAM, van Schie MH, Stehle G, de Bree R, Snow GB, Oyen WJG, van Dongen GAMS. Phase I therapy study with ^{186}Re-labeled humanized monoclonal antibody BIWA 4 (Bivatuzumab) in patients with head and neck squamous cell carcinoma. Clin Cancer Res 9:3961s-3972s, 2003.

Börjesson PKE, Postema EJ, de Bree R, Roos JC, Leemans CR, Kairemo KJA, van Dongen GAMS. Radioimmunodetection and radioimmunotherapy of head and neck cancer. Oral Oncol 40:761-772, 2004.

Chao KS, Deasy JO, Markman J, Haynie J, Perez CA, Purdy JA, Low DA. A prospective study of salivary function sparing in patients with head and neck cancers receiving intensity-modulated or three-dimensional radiation therapy: initial results. Int J Radiat Oncol Biol Phys 49(4):907-916, 2001.

Chappell PB, Leckman JF, Scahill LD, Hardin MT, Anderson G, Dohen DJ. Neuroendocrine and behavioural effects of the selective kappa agonist spiradoline in Tourette´s syndrome: a pilot study. Psychiatry Res 47:267-280, 1993.

Chen R, Aaltonen L-M and Vaheri A. Human papillomavirus type 16 in head and neck carcinogenesis. Rev Med Virol 15:351-363, 2005.

Chen Z, Nath R. Biologically effective dose (BED) for interstitial seed implants containing a mixture of radionuclides with different half-lifes. Int J Radiation Oncology Biol Phys 55(3):825-834, 2003.

Cheong N, Iliakis G. In vitro rejoining of double strand breaks induced in cellular DNA by bleomycin and restriction endonucleases. Int J Radiat Biol 71(4);365-375, 1997.

Chin D, Boyle GM, Porceddu S, Theile DR, Parsons PG, Coman WB. Head and neck cancer: past, present and future. Expert Rev Anticancer Ther 6(7):1111-1118, 2006.

Colnot DR, Nieuwenhuis EJC, Kuik DJ, Leemans CR, Dijkstra J, Snow GB, van Dongen GAMS, Brakendoff RH. Clinical significance of micrometastatic cells detected by E48 (Ly-6D) reverse transcription-polymerase chain reaction in bone marrow of head and neck cancer patients. Clin Cancer Res 10:7827-7833, 2004.

Constanzi JJ, Loukas D, Gagliano RG, Griffiths C, Barranco S. Intravenous bleomycin infusion as a potential synchronizing agent in human disseminated malignancies. A preliminary report. Cancer 38(4):1503-1506, 1976.

Cooper JS, Pajak TF, Forastiere AA, Jacobs J, Campbell BH, Saxman SB, Kish JA, Kim HE, Cmelak AJ, Rotman M, Machtay M, Ensley JF, Chao C, Schultz CJ, Lee N, Fu KK. Postoperative concurrent radiotherapy and chemotherapy for high-risk squamous-cell carcinoma of the head and neck. N Engl J Med 350:1937-1944, 2004.

Copper MP, Jovanovic A, Nauta JJ, Braakhuis BJM, de Vries N, Van der Waal DDS, Snow GB. Role of genetic factors in the etiology of squamous cell carcinoma of the head and neck. Arch Otolaryngol Head Neck Surg 121(2):157-160, 1995.

Corvò R. Evidence-based radiation oncology in head and neck squamous cell carcinoma. Radiother Oncol 85:156-170, 2007.

Crooke ST, Luft F, Broughton A, Strong J, Casson K, Einhorn L. Bleomycin serum pharmacokinetics as determinated by a radioimmunoassay and a microbiologic assay in a patient with compromised renal function. Cancer 39:1430-1434, 1977.

Dar ME, Jorgensen TJ. Deletions at short direct repeats and base substitutions are characteristic mutations for bleomycin-induced double- and single-strand breaks, respectively, in a human shuttle vector system. Nucleic Acids Res 23(16):3224-3230, 1995.

De Lanerolle NC, Williamson A, Meredith C, Kim JH, Tabuteau H, Spencer DD, Brines ML. Dynorphin and the kappa 1 ligand [^{3}H]U69,593 binding in the human epileptogenic hippocampus. Epilepsy Res 28:189-205, 1997.

DeNardo GL, Sysko VV, DeNardo SJ. Cure of incurable lymphoma. Int J Radiat Oncol Biol Phys 66(2):46s-56s, 2006.

De Stefani E, Deneo-Pellegrini H, Mendilaharsu M and Ronco A. Diet and risk cancer of the upper aerodigestive tract—I. Foods. Oral Oncol 35:17-21, 1999.

Ding M, Newman F, Raben D. New radiation therapy techniques for the treatment of head and neck cancer. Otolaryngol Clin North Am 38:371-395, 2005.

Domenge C, Orlowski S, Luboinski B, De Baere T, Schwaab G, Belehradek J, Jr, Mir LM. Antitumor electrochemotherapy: new advances in the clinical protocol. Cancer 77:956-963, 1996.

Dorr RT. Bleomycin pharmacology: Mechanism of action and resistance and clinical pharmacokinetics. Semin Oncol 19(2):3-8, 1992 .

Eisenberger M, Jacobs M. Simultaneous treatment with single-agent chemotherapy and radiation for locally advanced cancer of the head and neck. Semin Oncol 19(4 Suppl 11):41s-46s, 1992.

Elomaa L, Joensuu H, Kulmala J, Klemi P, Grénman R. Squamous cell carcinoma is highly sensitive to Taxol, a possible new radiation sensitizer. Acta Otolaryngol 115:340-344, 1995.

Elprana D, Kuijpers W, Wessels JMC, Wagener DJTh, van den Broek P. Chemosensitivity testing of xenografted squamous cell carcinomas of the head and neck region. Anticancer Res 12:2229-2240, 1992.

Erdogan MF, Gursoy A, Erdogan G, Kamel N. Radioactive iodine treatment in medullary thyroid carcinoma. Nucl Med Commun 27:359-362, 2006.

Erjala K, Pulkkinen J, Kulmala J, Grénman R. Concomitant vinorelbine and radiation in head and neck squamous cell carcinoma in vitro. Acta Otolaryngol 43(2):169-174, 2004.

Erjala K, Sundvall M, Junttila TT, Zhang NA, Savisalo M, Mali P, Kulmala J, Pulkkinen J, Grénman R, Elenius K. Signaling via ErbB2 and ErbB3 associates with resistance and Epidermal Growth Factor Receptor (EGFR) amplification with sensitivity to EGFR inhibitor gefitinib in head and neck squamous cell carcinoma cells. Clin Cancer Res 12(13):4103-4111, 2006.

Even-Sapir E, Bettman L, Iosilevsky G, Milshtein D, Frenkel A, Golodny GM, Ben-Haim S, Israel O, Front D. SPECT quantitation of cobolt-57-bleomycin to predict treatment response and outcome of patients with lung cancer. J Nucl Med 35:1129-1133, 1994.

Fakhry C, Gillison ML. Clinical implications of human papillomavirus in head and neck cancers. J Clin Oncol 24(17):2606-2611, 2006.

Faraggi M, Gardin I, de Labriolle-Vaylet C, Moretti JL, Bok BD. The influence of tracer localization on the electron dose rate delivered to the cell nucleus. J Nucl Med 35:113-119, 1994.

Finnist Cancer Registry 2006, www.cancerregistry.fi, visited May 22, 2008.

Fletcher GH, Evers WT. Radiotherapeutic management of surgical recurrences and postoperative residuals in tumors of the head and neck. Radiology 95:185-188, 1970.

Foulkes WD, Brunet JS, Kowalski LP, Narod SA, Franco EL. Family history of cancer is a risk factor for squamous cell carcinoma of the head and neck in Brazil: a case-control study. Int J Cancer 63:769-773, 1995.

Forastiere A, Koch W. Trotti A, Sidransky D. Head and neck cancer. N Engl J Med 345:1890-1900, 2001.

Forastiere AA, Goepfert H, Maor M, Pajak TF, Weber R, Morrison W, Glisson B, Trotti A, Ridge JA, Chao C, Peters G, Lee D-J, Leaf A, Ensley J, Cooper J. Concurrent chemotherapy and radiotherapy for organ preservation in advanced laryngeal cancer. N Engl J Med 349:2091-2098, 2003.

Fujimoto J. Autoradiographic studies on the intracellular distribution of bleomycin-14^{C} in mouse tumor cells. Cancer Res 34:2969-2974, 1974.

Fu KK, Phillips TL, Silverberg IJ, Jacobs C, Goffinet DR, Chun C, Friedman MA, Kohler M McWhirter K, Carter SK. Combined radiotherapy and chemotherapy with bleomycin and methotrexate for advanced inoperable head and neck cancer: update of a Northern California Oncology Group Randomized Trial. J Clin Oncol 5:1410-1418, 1987.

Gerretsen M, Visser GWM, van Walsum M, Meijer CJLM, Snow GB, van Dongen GAMS. ^{186}Re-labeled monoclonal antibody E48 immunoglobulin G-mediated therapy of human head and neck squamous cell carcinoma xenografts. Cancer Res 53:3524-3529, 1993.

Gibson MK, Forastiere AA. Multidisciplinary approaches in the management of advanced head and neck tumors: state of the art. Curr Opin Oncol 16:220-224, 2004.

GLOBOCAN 2002, www-dep.iarc.fr, visited May 20, 2008.

Goerres GW, Schmid DT, Bandhauer F. Positron emission tomography in the early follow-up of advanced head and neck cancer. Arch Otolaryngol Head Neck Surg 130:105-109, 2004.

Graham MM, Metter DF. Evolution of nuclear medicine training: past, present and future. J Nucl Med 48:257-268, 2007.

Grénman R, Burk D, Virolainen E, Wagner JJ, Lichter AS, Carey TE. Radiosensitivity of head and neck cancer cells *in vitro*: a 96-well-plate clonogenic assay for squamous cell carcinoma. Arch Otolaryng 114:427-431, 1988a.

Grénman R, Burk D, Virolainen E , Wagner JG. Radiosensitivity of head and neck cancer cells in vitro. Arch Otolaryngol Head Neck Surg 114:427-431, 1988b.

Grénman R, Burk D, Virolainen E, Buick RN, Church J, Schwatz DR, Carey TE. Clonogenic cell assay for anchorage-dependent squamous carcinoma cell lines using limiting dilution. Int J Cancer 44:131-136, 1989.

Grénman R, Carey TE, McClatchey KD, Wagner JG, Pekkola-Heino K, Schwartz DR, Wolf GT, Lacivita LP, Ho L, Baker SR, Krause CJ, Lichter AS. In vitro radiation resistance among cell lines established from patients with squamous cell carcinoma of the head and neck. Cancer 67:2741-2747, 1991.

Grimard L, Esche B, Lamothe A, Cygler J, Spaans J. Interstitial low-dose-rate brachytherapy in the treatment of recurrent head and neck malignancies. Head Neck 28:888-895, 2006.

Guggenheimer J, Verbin RS, Johson JT, Horkowitz CA, Myers EN. Factors delaying the diagnosis of oral and oropharyngeal carcinomas. Cancer 64:932-935, 1989.

Hiltunen JV, Kairemo KJA, Nikula TK. Pharmacokinetic properties of low pH In-111-bleomycin complex. In Advances in Radiopharmacology. Proceedings of the Sixth International Association of Radiopharmacology 1990, Sydney, Australia, edit. Maddalena D.J, Snowdon G.M, and Boniface G.R, Wollongong University Press Australia, 1990: 136-139.

Horiot JC, Le Fur R, N´Guyen T, Chenal C, Schraub S, Alfonsi S, Gardani G, Van Den Bogaert W, Danczak S, Bolla M, Van Glabbeke M, De Pauw M. Hyperfractionation versus conventional fractionation in oropharyngeal carcinoma: final analysis of a randomized trial of the EORTC cooperative group of radiotherapy. Radiother Oncol 25:231-241, 1992.

Horiot JC, Bontemps P, van den Bogaert W, Le Fur R, van den Weijngaert D, Bolla M, Bernier J, Lusinchi A, Stuschke M, Lopez-Torrecilla J, Begg AC, Pierart M, Collette L. Accelerated fractionation (AF) compared with conventional fractionation (CF) improves loco-regional control in the radiotherapy of advanced head and neck cancers of the EORTC 22851 randomized trial. Radiother Oncol 44:111-121, 1997.

Hou D-Y, Hoch H, Johnston GS, Tsou KC, Jones AE, Miller EE, Larson SM. A new tumor imaging agent – ^{111}In-bleomycin complex. Comparison with ^{67}Ga-citrate and ^{57}Co-bleomycin in tumor-bearing animals. J Surg Oncol 27:189-195, 1984a.

Hou D-Y, Hoch H, Johnston GS, Tsou KC, Jones AE, Farkas RJ, Miller EE. A new ^{111}In-bleomycin complex for tumor imaging: preparation, stability and distribution in glioma-bearing mice. J Surg Oncol 25:168-175, 1984b.

Hou D-Y, Hoch H, Johnston GS, Tsou KC, Jones AE, Farkas RJ, Miller EE, Larson SM. A new ^{111}In-bleomycin complex for combined radiotherapy and chemotherapy. J Surg Oncol 29:91-98, 1985.

Hou D-Y, Hamburger AW, Beach JL, Maruyama Y. Killing of human lung cancer cells using a new ^{111}In-bleomycin complex (^{111}InBLMC). Cancer Invest 7:543-550, 1989a.

Hou D-Y, Ordonez JV, Cross RJ, Ross DD, Mauyama Y. Killing lung cancer cells at cell-cycle phase by a new indium-111-bleomycin complex. J Surg Oncol 40:73-78, 1989b.

Hou D-Y, Maruyama Y. Distribution of ^{111}In-bleomycin complex in small cell lung cancer cells by autoradiography. J Surg Oncol 49:93-97, 1992.

Hou D-Y, Maruyama Y, Drago JR. Chromosome aberrations of human small cell lung cancer induced by a new ^{111}In-bleomycin complex. J Surg Oncol 51:236-242, 1992.

Howell RW, Rao DV, H D-Y, Narra VR, Sastry KSR. The question of relative biological effectiveness and quality factor for Auger emitters incorporated into proliferating mammalian cells. Radiat Res 128:282-292, 1991.

Howell RW. Radiation spectra for Auger-electron emitting radionuclides: report no.2 of AAPM nuclear medicine task group np.6. Med Phys 19(6):1371-1383, 1992.

Howell RW, Narra VR, Sastry KSR, Rao DV. On the equivalent dose for Auger electron emitters. Radiat Res 134:71-78, 1993.

Hsu SM, Raine L, Fanger H. Use of the avidin-biotin-peroxidase complex (ABC) in immunoperoxidase techniques: A comparison between ABC and unlabeled antibody (PAP) procedures. J Histochem Cytochem 29:577-580, 1981.

ICRP, Radionuclide Transformations: Energy and Intensity of Emissions, Publication 38. International Comission on Radiobiological Projection, Pergamon, New York, 1983.

ICRP, RBE for Deterministic Effects, Publication 58. International Comission on Radiobiological Projection, Pergamon, New York, 1990.

Iqbal ZM, Kohn KW, Ewig RAG, Fornace AJ Jr. Single-strand scission and repair of DNA in mammalian cells by bleomycin. Cancer Res 36:3834-3838, 1976.

Jacob R, Welkoborsky HJ, Mann WJ, Höfken F, Dienes H-P, Freije JE. Heterogeneity of squamous cell carcinomas of the head and neck – analysis of tumor biologic factors and proliferation rates. Laryngoscope 106:1170-1175, 1996.

Jalilian AR, Bineshmarvasti M, Sardari S. Application of radioisotopes in inflammation. Curr Med Chem 13(8):959-965, 2006.

Johns HE, Cunningham JR. The Physics of Radiology. Fourth Edition. Edit. Johns HE, Cunningham JR, Charles C Thomas · Publisher, Springfield, USA, 1983, pp 12-25.

Kairemo KJA, Ramsay H, Nikula TK, Hopsu EVM, Taavitsainen MJ, Bondestam S, Hiltunen JV. A low PH In-111-bleomycin complex (BLMC), a tracer for radiochemotherapy of head and neck cancer. J Nucl Med Biol 38(Suppl I):135-139, 1994.

Kairemo KJA, Ramsay HA, Paavonen T, Bondestam S. Imaging and staging of head and neck cancer using a low pH In-111-bleomycin complex. Oral Oncol, Eur J Cancer 32B(5):311-321, 1996a.

Kairemo KJA, Ramsay HA, Tagesson M, Jekunen AP, Paavonen TK, Jääskelä-Saari HA, Liewendahl K, Ljunggren K, Savolainen S, Strand S-E. Indium-111 bleomycin complex for radiochemotherapy of head and neck cancer – dosimetric and biokinetic aspects. Eur J Nucl Med 23(6):631-638, 1996b.

Kassis AI, Fayad F, Kinsey BM, Sastry KSR, Taube RA, Adelstein SJ. Radiotoxicity of ^{125}I in mammalian cells. Radiat Res 111:305-318, 1987a.

Kassis AI, Sastry KSR, Adelstein SJ. Kinetics of uptake, retention, and radiotoxicity of ^{125}IudR in mammalian cells: implications of localized energy deposition by Auger processes. Radiat Res 109:78-89: 1987b.

Kassis AI, Kirichian AM, Wang K, Safaie Semnani E, Adelstein SJ. Therapeutic potential of 5-[^{125}I]iodo-2′-deoxyuridine and methotrexate in the treatment of advanced neoplastic meningitis. Int J Radiat Biol 80:941-946, 2004.

Kassis AI. Radiotargeting agents for cancer therapy. Expert Opin Drug Deliv 2(6):981-991, 2005.

Kassis AI, Adelstein SJ. Radiobiologic principles in radionuclide therapy. J Nucl Med 46:4s-12s, 2005.

Kievit E, van Gog FB, Schlüper HMM, van Dongen GAMS, Pinedo HM, Boven E. Comparison of the biodistribution and the efficacy of monoclonal antibody 323/A3 labeled with either ^{131}I or ^{186}Re in human ovarian cancer xenografts. Int J Radiat Oncol Biol Phys 38(4):813-823, 1997.

Kohn KW, Ewig RA. Effect of ph on the bleomycin-induced DNA single-strand scission in L1210 cells and the relation to cell curvival. Cancer Res 36:3839-3841, 1976.

Korppi-Tommola T, Huhmar H, Aronen HJ, Penttilä P, Hiltunen J, Savolainen S, Kallio ME, Liewendahl K. ^{111}In-labelled bleomycin complex for the differentation of high- and low-grade gliomas. Nucl Med Commun 20(2):145-152, 1999.

Kramer WG, Feldman S, Broughton A, Strong JE, Hall SW, Hloye PY. The pharmacokinetics of bleomycin in man. J Clin Pharmacol 18:346-352, 1978.

Kraunz KS, Hsiung D, McClean MD, Liu M, Osanyingbemi J, Nelson HH, Kelsey KT. Dietary folate is associated with $p16^{INK4A}$ methylation in head and neck squamous cell carcinoma. Int J Cancer 119:1553-1557, 2006a.

Kraunz KS, McClean MD, Nelson HH, Peters E, Calderon H, Kelsey TK. Duration but not intensity of alcohol and tobacco exposure predicts $p16^{INK4A}$ homozygous deletion in head and neck squamous cell carcinoma. Cancer Res 66(8):4512-4515, 2006b.

Kuo MT, Haidle CW. Characterization of chain breakage in DNA induced by bleomycin. Biochem Biophys Acta 335:109-114, 1973.

Lansford CD, Grénman R, Bier H, Somers KD, Kim S-Y, Whiteside TL, Clayman GL, Welkoborsky H-J, Carey TE. Head and neck cancers. In Human Cell Culture Vol 2, Cancer Cell Lines Part 2. J. Edit. Masters and Palsson B., Kluwer Academic Press, Dordrecht Holland 1999: 185-255.

Laramore GE, Scott CB, al-Sarraf M, Haselow RE, Ervin TJ, Wheeler R, Jacobs JR, Schuller DE, Gahbauer RA, Schwade JG, Campbell BH. Adjuvant chemotherapy for respectable squamous cell carcinomas of the head and neck: report on Intergroup Study 0034. Int J Radiat Oncol Biol Phys 23:705-713, 1992.

Lazo JS, Boland CJ, Schwartz PE. Bleomycin hydrolase activity and cytotoxicity in human tumors. Cancer Res 42:4026-4031, 1982.

Leemans CR, Tiwari R, Nauta JJP, van der Waal I, Snow GB. Regional lymph node involvement and its significance in the development of distant metastases in head and neck carcinoma. Cancer 71:452-456, 1993.

Léon X, Quer M, Orús C, del Prado, Venegas M, López M. Distant metastases in head and neck cancer patients who achieved loco-regional control. Head Neck 22:680-686, 2000.

Ling CC. Permanent implants using Au-198, Pd-103 and I-125: radiobiological considerations based on the linear quadratic model. Int J Radiation Oncology Biol Phys 23(1):81-87, 1992.

Licitra L, Bernier J, Grandi C, Merlano M, Bruzzi P, Lefebvre JL. Cancer of the oropharynx. Crit Rev Oncol Hematol 41:107-122, 2002.

Ljunggren K and Strand S-E. Beta camera for statistic and dynamic imaging of charged-particle emitting radionuclides in biologic samples. J Nucl Med 31:2058-2063, 1990.

Ljungberg M, Strand S-E, Tagesson M. A treatment planning system for radionuclide therapy. Eur J Nucl Med 21:76s, 1994a.

Ljungberg M, King MA, Hademenos KG, Strand S-E. Comparison of four scatter correction methods using Monte Carlo simulated source distributions. J Nucl Med 35:143-151, 1994b.

Lown JW, Sim S. The mechanism of the bleomycin-induced cleavage of DNA. Biochim Biophys Res Commun 77:1150-1157, 1977.

Lu S-L, Herrington H, Wang X-J. Mouse models for human head and neck squamous cell carcinomas. Head Neck 28: 945-954, 2006.

Marsit CJ, McClean MD, Furniss CS, Kelsey KT. Epigenetic inactivation of the SFRP genes is associated with drinking, smoking and HPV in head and neck squamous cell carcinoma. Int J Cancer 119:1761-1766, 2006.

Mathieu-Kia AM, Fan LQ, Kreek MJ, Simon EJ, Hiller JM. μ-, δ- and κ-opioid receptor populations are differentially altered in distinct areas of postmortem brains of Alzheimer´s disease patients. Brain Res 893:121-134, 2001.

McLean JR, Blakey DH, Douglas GR, Bayley J. The Auger electron dosimetry of indium-111 in mammalian cells *in vitro.* Radiat Res 119:205-218, 1989.

Munro AJ. An overview of randomised controlled trials of adjuvant chemotherapy in head and neck cancer. Br J Cancer 71:83-91, 1995.

Murdoch D, Sager J. Will targeted therapy hold its promise? An evidence-based review. Curr Opin Oncol 20:104-111, 2008.

Narra VR, Sastry KSR, Goddu SM, Howell RW, Strand S-E, Rao DV. The relative biological effectiveness of ^{99m}Tc radiopharmaceuticals. Med Phys 21:1921-1926, 1994.
Nath R. New directions in radionuclide sources for brachytherapy. Semin Radiat Oncol 3(4):278-289, 1993.

Nose T, Koizumi M, Nishiyama K. High-dose-rate interstitial brachytherapy for oropharyngeal carcinoma: results of 83 lesions in 82 patients. Int J Radiat Oncol Biol Phys 59(4):983-991, 2004.

Nutting C, Horlock N, A´Hern R, Searle A, Henk JM, Rhys-Evans P, Harrington K. Manually after-loaded ^{192}Ir low-dose rate brachytherapy after subtotal excision and flap reconstruction of recurrent cervical lymphadenopathy from head and neck cancer. Radiother Oncol 80:39-42, 2006.

Ohnuma T, Holland JF, Masuda H, Waligunda JA, Goldberg GA. Microbiological assay of bleomycin: Inactivation, tissue distribution, and clearance. Cancer 33:1230-1238, 1974.

Orford J, Barker A, Thonell S, King P, Murphy J. Bleomycin therapy for cystic hygroma. J Pediatr Surg 30:1282-1287, 1995.

Paavonen T, Renkonen R. Selective expression of sialyl-Lewis x and Lewis a epitopes, putative ligands for L-selectin, on peripheral lymph-node high endothelial venules. Am J Pathol 141:1259-1264, 1992.

Parkin DM, Bray F, Ferlay J and Pisami P. Global cancer statistics, 2002. CA Cancer J Clin 55:74-108, 2005.

Pekkola-Heino K, Kulmala J, Grénman S, Carey TE, Grénman R. The radiation response of vulvar squamous cell carcinoma (UM-SCV-1A, UM-SCV-1B, M-SCV-2, A-431) cells in vitro. Cancer Res 49:4876-4878, 1989.

Pekkola-Heino K, Kulmala J, Klemi P, LakkalaT, Aitasalo K, Joensuu H, Grénman R. Effects of radiation fractionation on four squamous cell carcinoma lines with dissimilar inherent radiation sensitivity. J Cancer Res Clin Oncol 117:597-602, 1991.

Pekkola-Heino K, Kulmala J, Grénman R. Sublethal damage repair in squamous cell carcinoma cell lines. Head & Neck 14:196-199, 1992a.

Pekkola-Heino K, Kulmala J, Grénman R. Carboplatin-radiation interaction in squamous carcinoma cell lines. Arch Otolaryngol Head Neck Surg 118:1312-1315, 1992b.

Perk LR, Visser GWM, Vosjan MJWD, Stigter-van Walsum M, Tijink BM, Leemans CR, van Dongen GAMS. ^{89}Zr as a PET surrogate radioisotope for scouting biodistribution of the therapeutic radiometals ^{90}Y and ^{177}Lu in tumor-bearing nude mice after coupling to the internalising antibody cetuximab. J Nucl Med 46:1898-1906, 2005.

Perkins AC, Frier M. Radionuclide imaging in drug development. Curr Pharm Des 10:2907-2921, 2004.

Pernod M, Hoffstetter S, Peifferi D, Aletti P, Lapeyre M, Marchal C, Luporsi Surg 115:519-526, 1996.

Peters ES, McClean MD, Liu M, Eisen EA, Mueller N, Kelsey KT. The ADH1C polymorphism modifies the risk of squamous cell carcinoma of the head and neck associated with alcohol and tobacco use. Cancer Epidemiol Biomarkers Prev 14(2):476-482, 2005.

Pignon JP, Bourhis J, Domenge C, Designé L. Chemotherapy added to locoregional treatment for head and neck squamous-cell carcinoma: three meta-analyses of updated individual data. Lancet 355:949-955, 2000.

Pignon JP, Le Maître A, Bourhis J, on behalf of the MACH-NC Collaborative Group. Meta-analyses of chemotherapy in head and neck cancer (MACH-NC): an update. Int J Radiat Oncol Biol Phys 69(2):112s-114s, 2007.

Povirk LF, Han Y-H, Steighner RJ. Structure of bleomycin-induced DNA double-strand breaks: predominance of blunt ends and single-base 5´extensions. Biochemistry 28:5808-5814, 1989.

Pulkkinen J, Pekkola-Heino K, Grénamn R. Paclitaxel and irradiation induce apoptosis in squamous cell carcinoma cell lines in an additive way. Anticancer Res 16:2923-2930, 1996.

Puthawala A, Syed N, Gamie S, Chen Y-J, Londrc A, Nixon V. Interstitial low-dose-rate brachytherapy as a salvage treatment for recurrent head-and-neck cancers: long-term results. Int J Radiat Oncol Biol Phys 51(2):354-362, 2001.

Rao DV, Sastry KSR, Grimmond HE, Howell RW, Govelitz GF, Lanka VK, Mylavarapu VB. Cytotoxicity of some indium radiopharmaceuticals in mouse testes. J Nucl Med 29:275-384, 1988.

Rao DV, Narra VR, Howell RW, Sastry KSR. Biological consequence of nuclear versus cytoplasmic decays of ^{125}I: Cysteamine as a radioprotector against Auger cascades *in vivo.* Radiat Res 124:188-193, 1990.

Rao DV, Narra VR, Howell RW, Lanka VK, Sastry KSR. Induction of spermhead abnormalities by incorporated radionuclides: Dependence on subcellular distribution, type of radiation, dose rate, and presence of radioprotectors. Radiat Res 125:89-97, 1991.

Rufini V, Castaldi P, Treglia G, Perotti G, Gross MD, Al-Nahhas A, Rubello D. Nuclear medicine procedures in the diagnosis and therapy of medullary thyroid carcinoma. Biomed Pharmacother 62:139-146, 2008.

Saarilahti K, Kouri M, Collan J, Hämäläinen T, Atula T, Joensuu H, Tenhunen M. Intensity modulated radiotherapy for head and neck cancer: evidence for preserved salivary gland function. Radiother Oncol 74: 251-258, 2005.

Sasiadek M, Schlade-Bartusiak K, Zych M, Noga L, Czemarmazowicz H. Opposite responses in two DNA repair capacity tests in lymphocytes of head and neck cancer patients. J Appl Genet 43(4):525-534, 2002.

Sastry KSR, Rao DV. Dosimetry of low energy electrons. In Physics of Nuclear Medicine: Recent Advances. Edit. Rao DV, Chandra R, Graham M, AAPM, Medical Physics Monograph No.10, American Institute of Physics, 1984: 169-208.

Schmid DT, Stoeckli SJ, Bandhauer F. Impact of positron emission tomography on the initial staging and therapy in locoregional advanced squamous cell carcinoma of the head and neck. Laryngoscope 113:888-891, 2003.

Septi SM, Jani JP, Mistry JS, Gorelik E, Lazo JS. Metabolic inactivation: a mechanism of human tumor resistance to bleomycin. Cancer Res 51:227-232, 1991.

Sham E, Durand RE. Cell kinetics and repopulation parameters of irradiated xenograft tumours in SCID mice: comparison of two dose-fractionation regimens. Eur J Cancer 35(5):850-858, 1999.

Shanta V, Krishnamurthi S. Combined bleomycin and radiotherapy in oral cancer. Clin Radiol 31:617-620, 1980.

Silbersteib EB. Radionuclides and radiopharmaceuticals for 2005. J Nucl Med 46(5):13N-14N,26N, 2005.

Sinclair WK. Cyclic X-ray responses in mammalian cells in vitro. Radiat Res 33(3):620-643, 1968.

Smid L, Budihna M, Zakotnik B, Soba E, Strojan P, Fajdiga I, Zargi M, Oblak I, Dremelj M, LeSnicar H. Postoperative concomitant irradiation and chemotherapy with mitomycin C and bleomycin for advanced head and neck carcinoma. Int J Radiat Oncol Biol Phys 56(4):1055-1062, 2003.

Snyder WS, Fisher HL Jr, Ford MR, Warner GG. Estimates of absorbed fractions for monoenergetic photon sourcer uniformly distributed in various organs of a heterogenous phantom: MIRD pamphlet no. 5. J Nucl Med 10(3):7s-52s, 1969.

Sobin LH, Wittekind Ch. TNM classification of malignant tumors. 6th Edition. Edit. Sobin LH, Wittekind Ch, Wiley-Liss, New York, 2002: 19-56.

Sorenson JA, Phelps ME. Basic atomic and nuclear physics 1. In The Physics in Nuclear Medicine. Second Edition. Edit. Sorenson JA, Phelps ME, W.B Saunders Company, Philadelphia 1987: 1-21.

Spector JG, Sessions DG, Haughey BH, Chao KSC, Simpson J, El Mofty S, Perez CA. Delayed regional metastases, distant metastases, and second primary malignancies in squamous cell carcinomas of the larynx and hypopharynx. Laryngoscope 111(6):1079-1087, 2001.

St John MAR, Abemayor E, Wong DTW. Recent new approaches to the treatment of head and neck cancer. Anticancer Drugs 17:365-375, 2006.

Stabin M. MIRDOSE 3. Radiation International Dose Information Center, Institude for Science and Education, P.O. Box 17, Oak Ridge, TN 37831, USA

Sung MW, Chang SO, Choi JH, Kim JY. Bleomycin sclerotherapy in patients with congenital lymphatic malformation in the head and neck. Am J Otolaryngol 16:236-241, 1995.

Syrjänen S. Human papillomavirus (HPV) in head and neck cancer. J Clin Virol 32(1):59s-66s, 2005.

Tagesson M, Ljungberg M, Strand SE. A Monte-Carlo program converting activity distributions to absorbed dose distributions in a radionuclide treatment planning system. Acta Oncol 35(3):367-372, 1996

Tenhunen M, Collan J, Kouri M, Kangasmäki A, Heikkonen J, Kairemo K, Mäkitie A, Joensuu H, Saarilahti K. Scintigraphy in prediction of the salivary gland function after gland-sparing intensity modulated radiation therapy for head and neck cancer. Radiother Oncol 87:260-267, 2008.

Thakur ML, Mennick MV, Guanasekera SW. Some pharmacological aspects of new radiopharmaceutical 111-In-bleomycin. In Radiopharmaceuticals and Labelled Compounds, Vol.II (Vienna: IAEA) 1973: 183-193.

Thilly WG, Deluca JG, Furth EE, Hoppe H, Kaden DA, Krolewski JJ, Liber HL, Skopek TR, Slapnikoff SA, Tizard RJ, Penman BW. Gene-locus mutation assays in diploid human lymphoblast lines. In Chemical mutagens. Edit. De Serpes FJ, Hollaender A, Plenum Publishing, New York 1980: 6: 331-364.

Trotti A. Toxicity in head and neck cancer: a review of trends and issues. Int J Radiat Oncol Biol Phys 47:1-12, 2000.

Umezawa H, Maeda K, Takeuchi T, Okami Y. New antibiotics, bleomycin A and B. J Antibiot, Ser A 19:200-209, 1966a.

Umezawa H, Suhara Y, Takita F, Maeda K. Purification of bleomycins. J Antibiot, Ser A 19:210-215, 1966b.

Urade M, Ogura T, Mima T, Matsuya S. Establishment of human squamous carcinoma cell lines highly and minimally sensitive to bleomycin and analysis of factors involved in the sensitivity. Cancer 69:2589-2597, 1992.

Verhey LJ. Issues in optimization for planning of intensity-modulated radiation therapy. Semin Radiat Oncol 12(3):210-218, 2002.

Wahlberg P, Wennerberg J, Alm P, Björklund A, Trope C. The effect of continuous bleomycin infusion on the growth and cell kinetics of heterotransplanted squamous cell carcinoma of the head and neck. Anticancer Res 7:55-58, 1987.

Walker DM, Boey G, McDonald LA.The pathology of oral cancer. Pathology 35(5):376-383, 2003.

Walkdron C, Shafer W. Leukoplakia revisisted: a clinicopathologic study of 3256 oral leukoplakia. Cancer 36:1386-1392, 1975.

Warnakulasuriya S, Sutherland G, Scully C. Tobacco, oral cancer, and treatment of dependence. Oral Oncol 41:244-260, 2005.

Weichselbaum RR. Radioresistant and repair proficient cells may determine radiocurability in human tumors. Int J Radiat Oncol Biol Phys 12:637-639, 1986.

Wennerberg J. Bleomycin induced changes in growth and cell kinetics of a heterotransplanted squamous cell carcinoma of the head and neck. Anticancer Res 4:419-424, 1984.

Xia P, Lee N, Liu Y-M, Poon I, Weinberg V, Shin E, Quivey JM, Verhey LJ. A study of planning dose constraints for treatment of nasopharyngeal carcinoma using a commercial inverse treatment planning system. Int J Radiat Oncol Biol Phys 59(3):886-96, 2004.

Zabro RJ, Crissman JD. The surgical pathology of head and neck cancer. Semin Oncol 15(1):10-19, 1988.